

THE FLORIDA STATE UNIVERSITY
COLLEGE OF ARTS AND SCIENCES

SOME INACCURACIES IN FINITE DIFFERENCING
HYPERBOLIC EQUATIONS

By

RICHARD GROTJAHN

A thesis submitted to the
Department of Meteorology
in partial fulfillment of
the requirements for the
degree of Master of Science.

Approved:

James L. Brown
Professor Directing Thesis

S. J. Blumsohn

August, 1975

T. N. Kishore Murthy

August, 1975

T. N. Kishore Murthy

ABSTRACT

The errors introduced by the use of various numerical schemes for solving mathematical models have generally been only vaguely determined previously by numerical modelers. A method for a more quantitative analysis of the inaccuracies is outlined. The error associated with some simple schemes is analyzed for several linear hyperbolic systems representative of typical problems in meteorology and oceanography. Results of previous studies of phase velocity inaccuracies are confirmed and form a basis for an extension of the analysis to group velocities. Significant angular and magnitude errors are found in the group velocity. Directional errors of 180° are found for some waves. Since the group velocity is the propagation speed of the energy, such errors may have severe consequences in a numerical model. When analysis was made of complex systems of equations, results found for simple systems reappeared. Thus, studies of simple systems may provide useful indications of behavior in more complex problems where the analysis may have to be limited. Only the long waves, i.e., those resolved by many grid points, are represented with any reasonable accuracy.

points, are represented with any reasonable accuracy.

ACKNOWLEDGMENTS

I wish to express my sincere gratitude to Dr. James J. O'Brien who, as my major professor, made several pivotal contributions and sacrificed much to expedite this work.

I would like to thank Dr. Steven Blumsack for serving on my committee and for providing help with some of the more subtle mathematical features of this research. I wish to thank Dr. T. N. Krishnamurti for also serving on my committee.

I acknowledge the generous correspondence and discussions from Drs. James Holton, André Robert, Arne Sundström, Richard Anthes, Joseph Gerrity, Svante Bodin, Albert Barcilon, Paul Swarztrauber, Harley Hurlburt, Dana Thompson and Norman Phillips. I also appreciate the help provided by Monty Peffley.

This Master's degree work was supported by the Office of Naval Research. Funds were also provided by the Coastal Upwelling Ecosystems Analysis Program, a program of the International Decade of Ocean Exploration under sponsorship of the National Science Foundation, Grants GX-33502 and ID075-06469.

Some of the graphics were produced using the Florida State University Computing Center CDC 6500.

Thanks are due to Sandra Jensen for typing the draft state University Computing Center CDC 6500.

Thanks are due to Sandra Jensen for typing the draft version of this paper, and to Janina Richards for typing the final manuscript.

TABLE OF CONTENTS

	Page
ABSTRACT	ii
ACKNOWLEDGMENTS	iii
LIST OF SYMBOLS	v
LIST OF ILLUSTRATIONS	vii
1. INTRODUCTION	1
2. METHOD	6
3. SIMPLE SYSTEMS	10
4. COMPLEX SYSTEMS	31
5. CONCLUSIONS	51
APPENDIX 1	53
APPENDIX 2	55
REFERENCES	63
VITA	65

LIST OF SYMBOLS

A	subscript "analytical"
C_g	group velocity
E	subscript "explicit"
f	Coriolis parameter (variable)
f_0	Coriolis parameter (constant)
I	subscript "implicit"
j	grid index, x direction
k	wavenumber, x direction
l	wavenumber, y direction
m	grid index, y direction
n	time level index
SI	subscript "semi-implicit"
u	x velocity
U	mean state velocity, x direction
v	y velocity
V	mean state velocity, y direction
β	first meridional derivative of f
Δt	time step
Δx	grid increment, x direction
Δy	grid increment, y direction
n	mode number in y direction
Δy	grid increment, y direction
n	mode number in y direction

λ	wavelength
Λ	dimensionless CFL parameter
ϕ	geopotential
Φ	mean state geopotential
ψ	streamfunction
ω	phase frequency

LIST OF ILLUSTRATIONS

Figure	Page
<p>1. Frequencies for the explicit and implicit schemes normalized by the correct frequency as a function of the nondimensional parameter $f\Delta t$. The explicit scheme overestimates the oscillation, whereas the implicit scheme underestimates it</p>	12
<p>2. Comparison of the two finite difference approximations to a first derivative in space, normalized by the correct value, as a function of wavenumber. λ is the corresponding wavelength in terms of grid intervals (i.e., when $k\Delta x = \pi/2$ the wavelength is $4\Delta x$)</p>	14
<p>3. Accuracy of the (a) explicit and (b) implicit phase frequencies for the advection equation as a function of the CFL parameter Λ. The limit for linear stability is $\Lambda = 1$. For $\Lambda < 1$ the two schemes are nearly the same; for $\Lambda > 1$ the implicit scheme maintains stability by slowing down the waves</p>	17
<p>4. Three characteristic curves originating from the point A, superimposed on a grid point lattice. The $\Lambda < 1$ curve is stable, the $\Lambda > 1$ curve is linearly unstable for an explicit formulation. For the explicit formulation used, the characteristic $\Lambda = 1$ is predicted exactly</p>	18
<p>5. Comparison of the phase velocity for the implicit formulation to the largest possible phase velocity for stability as a function of wavenumber for various values of Λ. The implicit scheme slows the waves down more than would be required to maintain stability, the limit is only asymptotically approached</p>	20
<p>than would be required to maintain stability, the limit is only asymptotically approached</p>	20

Figure	Page
6. Group velocities for the one-dimensional advection equation. Velocities of the two numerical schemes are normalized by the analytical value. The explicit scheme is always more accurate than the implicit for waves longer than $4\Delta x$. For waves shorter than $4\Delta x$, the energy in those wavelengths is propagated by both schemes in the opposite direction to the correct group velocity	21
7. Comparison of the group velocities between a so-called "fourth order" scheme and the "second order", centered-in-space scheme as a function of wavenumber. Long waves are treated quite well by the higher order scheme, however its treatment of the shortest waves is inferior to the second order scheme	23
8. Contour plots of the phase frequency for the two-dimensional (a) gravity waves system and (b) advection equation. The frequencies are normalized by the analytical solutions for various values of the x and y wavenumbers, k and ℓ	25
9. x component of the vector group velocity of the gravity waves for the explicit scheme, at $\Lambda = 0.5$. The contours are normalized by the correct group velocity	27
10. Same as Fig. 9 except for the implicit scheme for $\Lambda = 10$	28
11. Contour plots of the angular error in the vector group velocity of the numerical schemes measured positive counterclockwise from the correct direction for the two-dimensional (a) gravity waves system and (b) advection equation. Lines in (b) do not intersect the axes since the problem changes character there	30
12. Contours of the phase frequency of the inertia-gravity waves in the semi-implicit scheme normalized by the analytical frequency for $\Lambda = 0.5$. This figure is consistent with the contours for the phase frequency of the inertia-gravity waves in the semi-implicit scheme normalized by the analytical frequency for $\Lambda = 0.5$. This figure is consistent with the results from the gravity wave system treated in Section 3	33

Figure	Page
13. x component of the vector group velocity of the semi-implicit case normalized by the correct value for $\Lambda \sim 10$. Note similarity to the pure gravity wave case presented in Fig. 10	35
14. Phase velocity for the numerical treatment of the nondivergent barotropic vorticity equation normalized by the correct velocity of the Rossby waves	40
15. Contour plot of the directional error in the vector group velocity for the numerical formulations of the vorticity equation. The x components of the correct and numerical group velocities are zero along the dashed and dot-dashed lines, respectively	42
16. Plot of the magnitude of the group velocity for the numerical schemes normalized by the correct value	43
17. Phase velocity for the explicit formulation ($\Lambda = 0.5$) of the equatorial β -plane system normalized by the correct speeds. (E) is the eastward propagating gravity wave, (W) the westward propagating gravity wave and (R) the Rossby-Haurwitz wave. The insert shows the details of the error at small values of k. The analytical solution is complex for $\sim 1 \times 10^{-7} < k < 5 \times 10^{-7} \text{ m}^{-1}$ for $\beta = 10^{-11} \text{ m}^{-1} \text{ s}^{-1}$ and $\phi = 104 \text{ m}^2 \text{ s}^{-1}$, here $\Delta x = 10^5 \text{ m}$	48
18. Same as Fig. 17 but for the implicit scheme at $\Lambda \approx 5$. Note that the tenfold increase in Λ had little effect on the Rossby-Haurwitz waves. These results are consistent with previous results for simpler systems	49

1. INTRODUCTION

In order to study some real physical system, a scientist will often represent that system in a mathematical sense. This may be a collection of numbers which he labels observations or an equation or system of equations which he employs as a model. In proceeding from the real system to the mathematical model, assumptions and approximations were made which introduced a certain amount of error. In many geophysical problems, analytical tools are incapable of solving the equations in the model. Therefore, numerical techniques may have to be invoked which will introduce additional distortion into the representation. If the numerical techniques are carried out on a computer, there is the round off error inherent to the truncated arithmetic. The first and last aspects of the total error are generally well recognized and documented. However, the error created by approximating continuous differential equations with discrete algebraic ones is generally not known in detail by the numerical modeler. This lack of knowledge concerning the error introduced by finite differencing provided the impetus for this work.

impetus for this work.

This report will examine the error in finite differencing, which we call truncation error, in specific detail

for several linear systems derived from the "shallow water" primitive equations. It will be demonstrated that the true nature of the truncation error is not revealed in nebulous statements concerning the order of a Taylor series expansion; that descriptions such as " $O(\Delta t^2)$ " are grossly deficient and that more precise analysis is imperative.

The method of analysis used here has its roots in the classical stability analyses of Courant et al. (1928) and its extension by von Neumann (e.g., Charney et al., 1950). From the continuous equations the form of the analytic solution is determined. From this analytic form an appropriate discrete form of the solution is derived. These are substituted into the continuous and finite differenced equations, respectively, and the physically correspondent solutions are compared. For wave type solutions (which form the bulk of the solutions derived here) this results in a constraint upon the phase frequencies. Any phase or amplitude disparities between the continuous and discrete sets of equations can be deduced by comparing the respective frequencies.

Most previous studies of the error have been more or less empirical in nature (e.g., Orzag, 1971), however, a few quantitative analyses have been made. Those of Kurihara (1965) and Kwizak (1970) are of particular interest here. Kurihara was concerned with testing several implicit and iterative formulations on rather simplified equations. He Kurihara was concerned with testing several implicit and iterative formulations on rather simplified equations. He also considered the computational modes which appear in

three time level schemes. Kwizak applied Kurihara's method to a semi-implicit formulation and used an approach similar to the one used here, to analyze some common space and time differencing formulations. Elvius and Sundström (1973) wrote the f-plane shallow water primitive equations in matrix form, determined the eigenvectors and eigenfrequencies, and compared them with the continuous solutions. This method is more complete in that boundary conditions could be explicitly included but, as we shall see, in more complex systems there is some ambiguity introduced when the eigenvalues can only be found numerically. Their main concern was the proper choice of boundary conditions for various efficient semi-implicit staggered grid formulations. The work of Baer and Simmons (1970) for nonlinear, essentially spectral, equations involved testing several schemes for stability and also conservation of integral constraints. They found that there may be large amplitude errors which cancel out in the computation of the integral properties. Thus truncation error could not be necessarily determined from a scheme's conservative properties. Young (1968) tested many schemes on the spectral equations and also concluded that truncation error bore little relation to the order of the scheme chosen. However, he chose not to pursue the details of the truncation error.

It was decided that the emphasis here would not be the details of the truncation error.

It was decided that the emphasis here would not be upon testing many schemes (e.g., Grammelvedt, 1969).

Neither would various boundary or staggered grid formulations be emphasized - there are simply too many. The problem would become too specialized. Instead, some simple commonly used schemes are applied to several hyperbolic systems and analyzed away from the boundaries. More specific applications are left to the reader. The purpose here is to outline a way to determine quantitatively the error and to present what appear to be some general properties of it.

Some of the results presented here can be found in previous work (Kwizak, 1970). They are included for completeness. What represents new work is the study of more complex systems and comparisons of group velocities. The group velocity is perhaps a more important quantity than the phase velocity, in that energy is propagated at the group velocity.

It will be shown that explicit time differencing tends to speed up oscillations whereas implicit formulations slow them down. Space differencing makes non-dispersive waves dispersive. It also uniformly slows down the phase velocities, with the error increasing for shorter wavelengths. The group velocity for some wavelengths can be in the opposite direction of the correct group velocity. However, long waves, i.e. those resolved by many (> 10) grid points, are generally handled reasonably well. Properties evident in simple systems reappear when the schemes are applied to complex systems of equations with similar types

of solutions. This may be a useful approximation to a scheme's behavior in more complicated systems, since the method is found to have limitations when applied to those more complicated systems.

It is the author's belief that more precise knowledge of the error will lead to improvements upon it and that more elegant schemes can be formulated which are based on explicit knowledge of the error. At the least, a more judicious choice of a scheme can be made (e.g. Kreiss and Olinger, 1972). It may even be possible to employ the error itself in improving the scheme.

2. METHOD

The continuous differential equations are approximated by discrete algebraic (finite differenced) ones. The solution to the continuous equations is given by a function. The solution to the discrete equations is also given by a function. It is these two functions, both analytically derived, which are compared. Requiring an analytical solution to the differential equations means that we are dealing with equations which are never solved numerically! However, one chooses a solvable model which is similar to the more realistic model of interest, and the analysis of the former is applied, with some care, to the latter. In this report all the equations have been linearized so as to study the error in the scheme without the added complication of nonlinear effects. One might reasonably expect that one formulation judged superior to another via linear analysis would perform better than the other in a similar problem containing some degree of nonlinearity.

Many of the solutions derived here are propagating waves. The continuous solutions for a one dimensional problem have the form

waves. The continuous solutions for a one dimensional problem have the form

$$S_A = e^{i(kx - \omega t)} \quad (1)$$

where k is wavenumber in the x direction and ω is the phase frequency. The appropriate general solution for the differenced system is easily found

$$S_j = e^{i(kj\Delta x - \omega n\Delta t)} \quad (2)$$

where j is an index in the x direction, Δx is the spatial grid interval, n is a time step index and Δt is the time step. The form (2) is appropriate because it will have the same functional form when substituted into the discrete equations as (1) has when substituted into the differential set. To see this more clearly, consider the first derivative of each solution:

$$\frac{\partial}{\partial x} (S_A) = ikS_A \quad (3)$$

$$\frac{1}{2\Delta x} (S_{j+1} - S_{j-1}) = i \frac{\sin k\Delta x}{\Delta x} S_j \quad (4)$$

where subscripts in (4) refer to a grid point. Just as there is no x dependence in the coefficient multiplying S_A on the right hand side of (3), there is no x dependence in the coefficient multiplying S_j in (4). That is, (3) and (4) have the same functional form.

One cannot always form the discrete analog this easily. For example, one of the problems treated later has a solution of the form

$$S_A = e^{x^2}$$

then

$$S_A = e^{x^4}$$

then

$$\frac{\partial}{\partial x} (S_A) = 2xe^{x^2} \quad (5)$$

Note that finite differencing a solution

$$S_j = e^{(j\Delta x)^2} \quad (6)$$

leads to

$$\frac{1}{2\Delta x} (S_{j+1} - S_{j-1}) = \frac{1}{\Delta x} \sinh (2j\Delta x^2) e^{\Delta x^2} S_j$$

This does not have the same functional form as (5). To be strictly correct one must resort to an eigenvector analysis in such a case. In the particular problem considered later, it was allowable to use the form (6) despite being inexact, because (6) was close to the correct solution.

Substitution of (1) and (2) into their respective systems yields dispersion relations from which the phase frequencies of the two systems are derived as a function of relevant parameters. The phase error is thereby deduced as a function of those parameters.

For solutions whose temporal dependence is $\exp(i\omega n\Delta t)$, the function for ω will involve either the arcsine or arctangent of some quantity. This presents an infinite number of frequencies, each shifted by some increment of π . Only those values of the inverse transcendentals between $-\pi/2$ and $\pi/2$ will be considered. This is justified since as the time and space increments approach zero, the finite differenced solution for ω will approach the true solution, not one shifted by some increment of π .
finite differenced solution for ω will approach the true solution, not one shifted by some increment of π .

The group velocities are obtained by differentiating the phase frequencies with respect to wavenumber. This

will be used as an indication of how the energy contained in different wavenumbers is propagating. An excellent review of the physics of the group velocity is provided by Whitham (1974).

It should be noted that the imaginary part of the phase frequency will imply growth (or decay). If the analytical frequency is real and the finite differenced frequency complex, then there will be amplitude errors as well, in the numerical scheme chosen.

In this study various combinations of the "shallow water" primitive equations will be used. Some simple systems with only one distinct solution will be considered first. Many of these results will reappear when systems with multiple roots and non-constant coefficients are examined.

3. SIMPLE SYSTEMS

There are two basic approaches to time differencing, either explicit or implicit formulations. We will treat both. In the more complex systems they will be mixed.

As an example of an ordinary differential equation in time, consider inertial oscillations. If we define

$$w \equiv u + iv$$

then our model is

$$w_t = -ifw \quad (7)$$

The solution to (7) is

$$w = e^{i\omega t}$$

where

$$\omega_A = -f \quad (8)$$

An explicit formulation of (7) is

$$w^{n+1} = w^{n-1} - 2if \Delta t w^n \quad (9)$$

where superscripts refer to the time level. Substitution into (9) of a solution of the form

$$w = D e^{i\omega n \Delta t}$$

yields

$$D e^{i\omega (n+1) \Delta t} = D e^{i\omega (n-1) \Delta t} - 2if \Delta t D e^{i\omega n \Delta t}$$

yields

$$\omega_E = -\frac{1}{\Delta t} \arcsin (f\Delta t) \quad (10)$$

For an implicit formulation

$$w^{n+1} = w^n - \frac{i\Delta t}{2} (w^n + w^{n+1})$$

one obtains a phase frequency

$$\omega_I = - \frac{2}{\Delta t} \arctan \left(\frac{f\Delta t}{2} \right) \quad (11)$$

The ratios of the physical solutions in (10) and (11), normalized by (8), are plotted in Fig. 1 as a function of the nondimensional parameter $f\Delta t$. The explicit formulation is tending to overestimate the oscillation whereas the implicit treatment is underestimating it. The explicit formulation is unstable for $f\Delta t > 1$. As the time step increases the two schemes diverge from the correct value.

It is interesting to note that in such a linear problem one could achieve quite high accuracy, while retaining large time increments, through a judicious mixture of explicit and implicit integrations. That is, one could nullify the overestimation of an explicit formulation by following with an implicit scheme. For a nonlinear model, such as the spectral equations, this technique may be useful, though two problems remain. The time steps would probably still need to be relatively small so as not to miss too much of the nonlinear effects during any given time step. Also a useful implicit scheme which avoids iteration would be preferred.

Before proceeding to problems with mixed time and space derivatives, consider space differentiation singly.

Before proceeding to problems with mixed time and space derivatives, consider space differentiation singly. For a wave type solution,

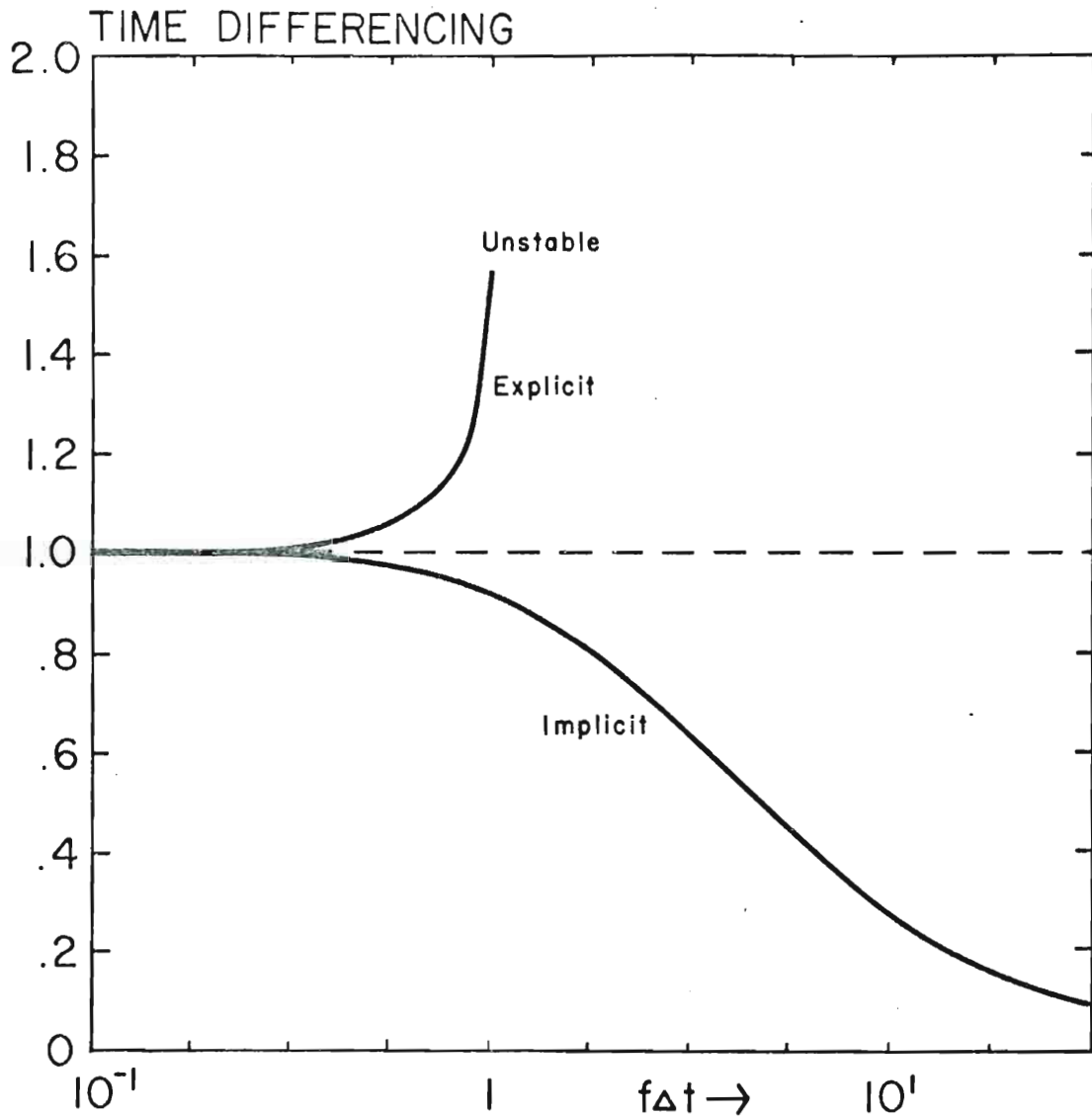


Fig. 1. Frequencies for the explicit and implicit schemes normalized by the correct frequency as a function of the nondimensional parameter $f\Delta t$. The explicit scheme overestimates the oscillation, whereas the implicit scheme underestimates it.

$$\frac{\partial}{\partial x} e^{(ikx)} = ik e^{ikx}$$

and for a centered-in-space finite difference approximation,

$$\frac{1}{2\Delta x} (e^{ik(j+1)\Delta x} - e^{ik(j-1)\Delta x}) = \frac{i \sin k\Delta x}{\Delta x} e^{ikj\Delta x} \quad (12)$$

In a sense there is a "computational wavenumber", $\sin k\Delta x/\Delta x$, corresponding to the true wavenumber, k . This implies that the representation is fairly good for long waves (i.e., those resolved by many grid points) but quite poor for shorter waves, particularly those less than $4\Delta x$. (Note: a $4\Delta x$ wavelength corresponds to $k\Delta x = \pi/2$). A fourth order scheme is

$$\begin{aligned} \frac{1}{\Delta x} \left[\frac{2}{3} (e^{ik(j+1)\Delta x} - e^{ik(j-1)\Delta x}) - \frac{1}{12} (e^{ik(j+2)\Delta x} - e^{ik(j-2)\Delta x}) \right] \\ = i \left(\frac{8 \sin k\Delta x - \sin 2k\Delta x}{6\Delta x} \right) e^{ikj\Delta x} \quad (13) \end{aligned}$$

The relations (12) and (13), normalized by the correct value k are both plotted in Fig. 2. The five point scheme is clearly superior to the centered-in-space formulation for all wavenumbers.

Consider the simple advection equation

$$\phi_t + U\phi_x + V\phi_y = 0 \quad (14)$$

where U and V are constant basic state velocities in the x and y directions, respectively. For a solution of the form

$$\phi = e^{i(kx + \ell y - \omega_A t)} \quad (15)$$

$$\phi = e^{i(kx + \ell y - \omega_A t)} \quad (15)$$

one obtains the constraint

$$\omega_A = Uk + V\ell \quad (16)$$

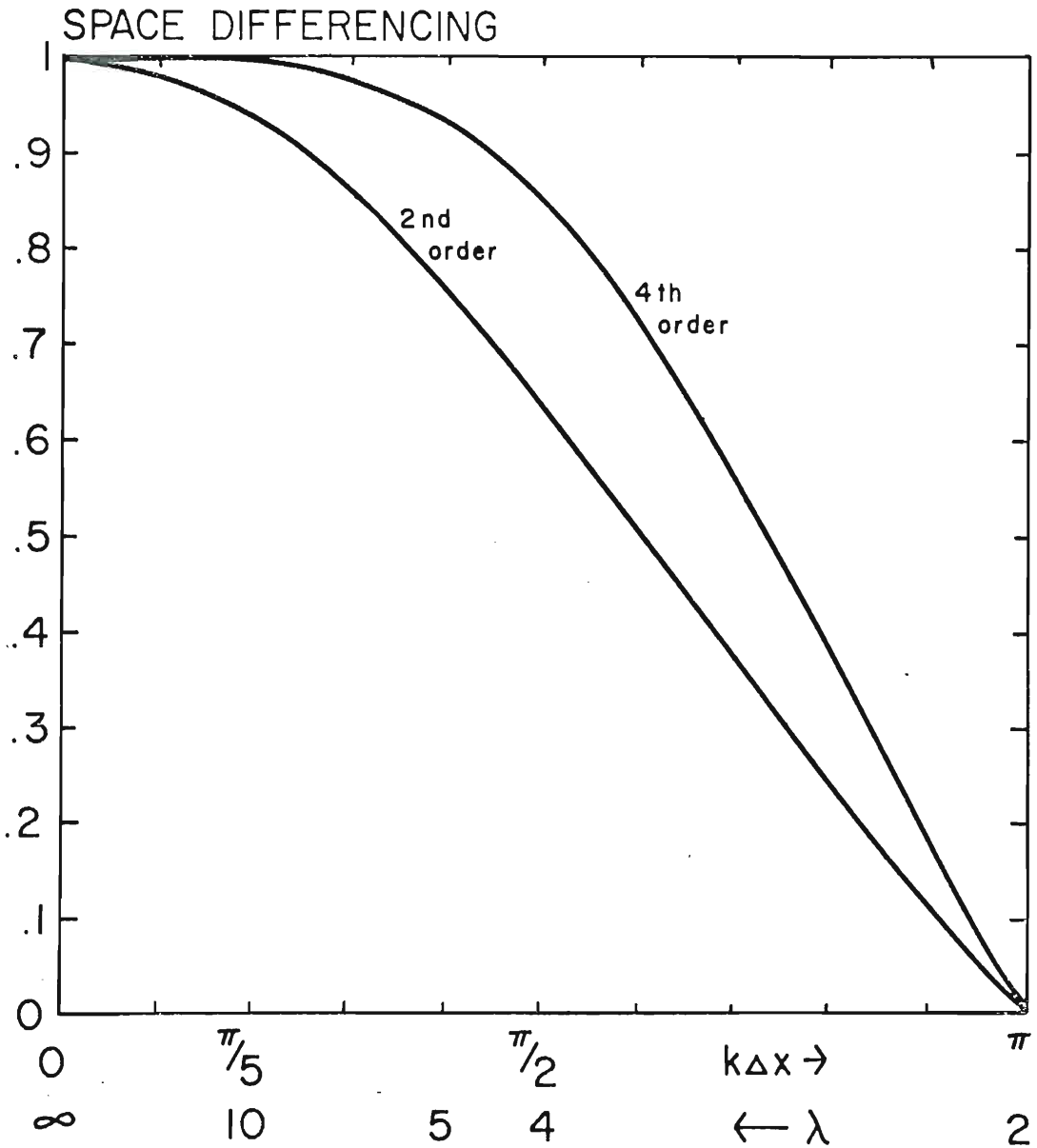


Fig. 2. Comparison of the two finite difference approximations to a first derivative in space, normalized by the correct value, as a function of wavenumber. λ is the corresponding wavelength in terms of grid intervals (i.e., where $k\Delta x = \pi/2$ wavelength is $4\Delta x$).

normalized by the correct value, as a function of wavenumber. λ is the corresponding wavelength in terms of grid intervals (i.e., where $k\Delta x = \pi/2$ wavelength is $4\Delta x$).

An explicit formulation of (14) is

$$\phi^{n+1} = \phi^{n-1} - U \frac{\Delta t}{\Delta x} \left(\phi_{j+1}^n - \phi_{j-1}^n \right) - V \frac{\Delta t}{\Delta y} \left(\phi_{m+1}^n - \phi_{m-1}^n \right)$$

which, when the solution

$$\phi^n = e^{i(kj\Delta x - \ell m\Delta y - \omega_E n\Delta t)} \quad (17)$$

is inserted, reveals

$$\omega_E = \frac{1}{\Delta t} \arcsin \left[U \frac{\Delta t}{\Delta x} \sin k\Delta x + V \frac{\Delta t}{\Delta y} \sin \ell\Delta y \right] \quad (18)$$

Substitution of (17) into an implicit formulation

$$\begin{aligned} \phi^{n+1} = \phi^n - U \frac{\Delta t}{4\Delta x} & \left(\phi_{j+1}^n + \phi_{j+1}^{n+1} - \phi_{j-1}^n - \phi_{j-1}^{n+1} \right) \\ & - V \frac{\Delta t}{4\Delta y} \left(\phi_{m+1}^n + \phi_{m+1}^{n+1} - \phi_{m-1}^n - \phi_{m-1}^{n+1} \right) \end{aligned}$$

yields

$$\omega_I = \frac{2}{\Delta t} \arctan \left[U \frac{\Delta t}{2\Delta x} \sin k\Delta x + V \frac{\Delta t}{2\Delta y} \sin \ell\Delta y \right] \quad (19)$$

Appendix 1 outlines these derivations in detail.

The explicit phase frequency (18) is compared to the continuous one, (16), Fig. 3, for various values of Λ . Here Λ is the nondimensional ratio

$$\Lambda = U \frac{\Delta t}{\Delta x}$$

$\Lambda = 1$ is the Courant-Friedrichs-Lewy (CFL) condition for linear stability. There are two aspects of the curves worth noting. The characteristic shape is similar to that in Fig. 1. There are two aspects of the curves worth noting. The characteristic shape is similar to that in Fig. 2. The waves have been made dispersive (the phase velocity depends on the wavenumber) by the finite differencing process,

with the representation poorer for shorter waves. At the CFL condition the phase frequency is exact for waves longer than $4\Delta x$. This is due to the characteristics of the continuous system intersecting the grid points as indicated by the $\Lambda = 1$ curve in Fig. 4. The true value at the point A'' is that at the point A' . If one writes the centered-in-space difference as

$$A'' = B - \Lambda (B' - A')$$

then for $\Lambda = 1$, B' is the value at B and the difference reduces to $A'' = A'$ which is the true solution. The fact that waves smaller than $4\Delta x$ appear to be treated poorly is due in part to our use of only the first harmonic of the arcsine (values between $-\pi/2$ and $\pi/2$). Since at $\Lambda = 1$ we are computing

$$\arcsine(\sin k\Delta x),$$

we are therefore not retrieving $k\Delta x$ for $k\Delta x > \pi/2$. This slight ambiguity concerning the arcsine in deriving the phase frequencies was apparently not recognized by previous investigators. However, in actual computer tests, the choice of arcsine values between $-\pi/2$ and $\pi/2$ appears to be proper. Note that there is no such ambiguity in the computation of the group velocities.

For $\Lambda = 1$, the implicit formulation (see Fig. 3) is very close to the explicit scheme in terms of accuracy (but for $\Lambda = 1$, the implicit formulation (see Fig. 3) is very close to the explicit scheme in terms of accuracy (but just slightly worse). For $\Lambda > 1$, the explicit scheme is unstable, whereas the implicit scheme maintains stability

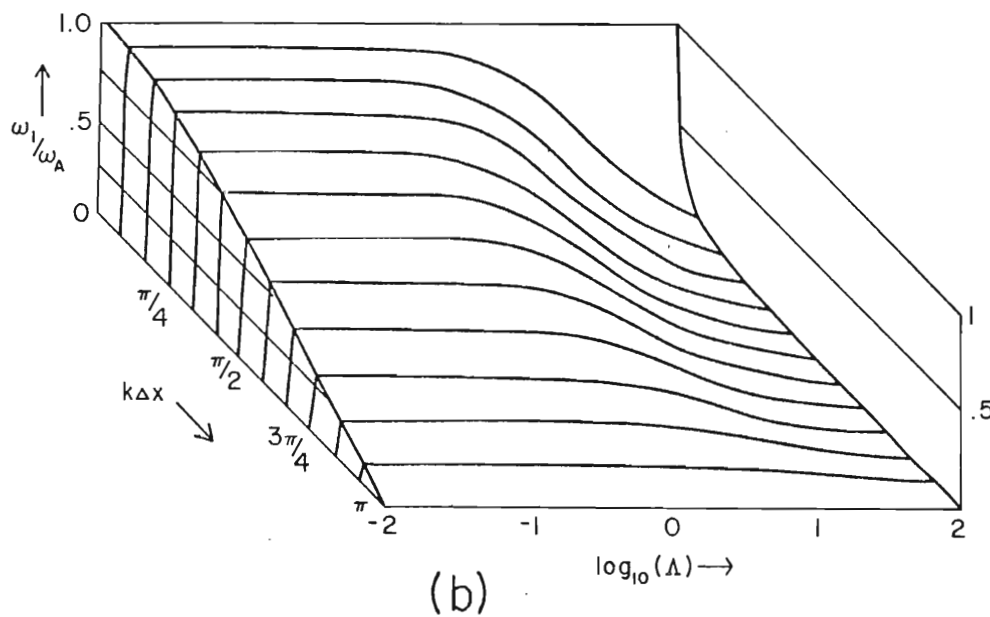
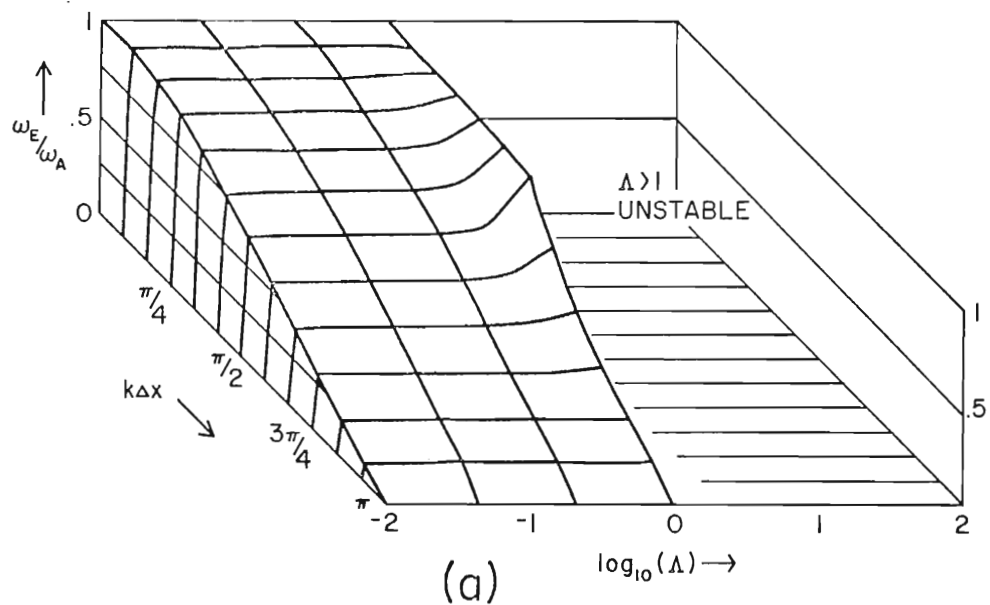


Fig. 3. Accuracy of the (a) explicit and (b) implicit

Fig. 3. Accuracy of the (a) explicit and (b) implicit phase frequencies for the advection equation as a function of the CFL parameter Λ . The limit for linear stability is $\Lambda = 1$. For $\Lambda < 1$ the two schemes are nearly the same; for $\Lambda > 1$ the implicit scheme maintains stability by slowing down the waves.

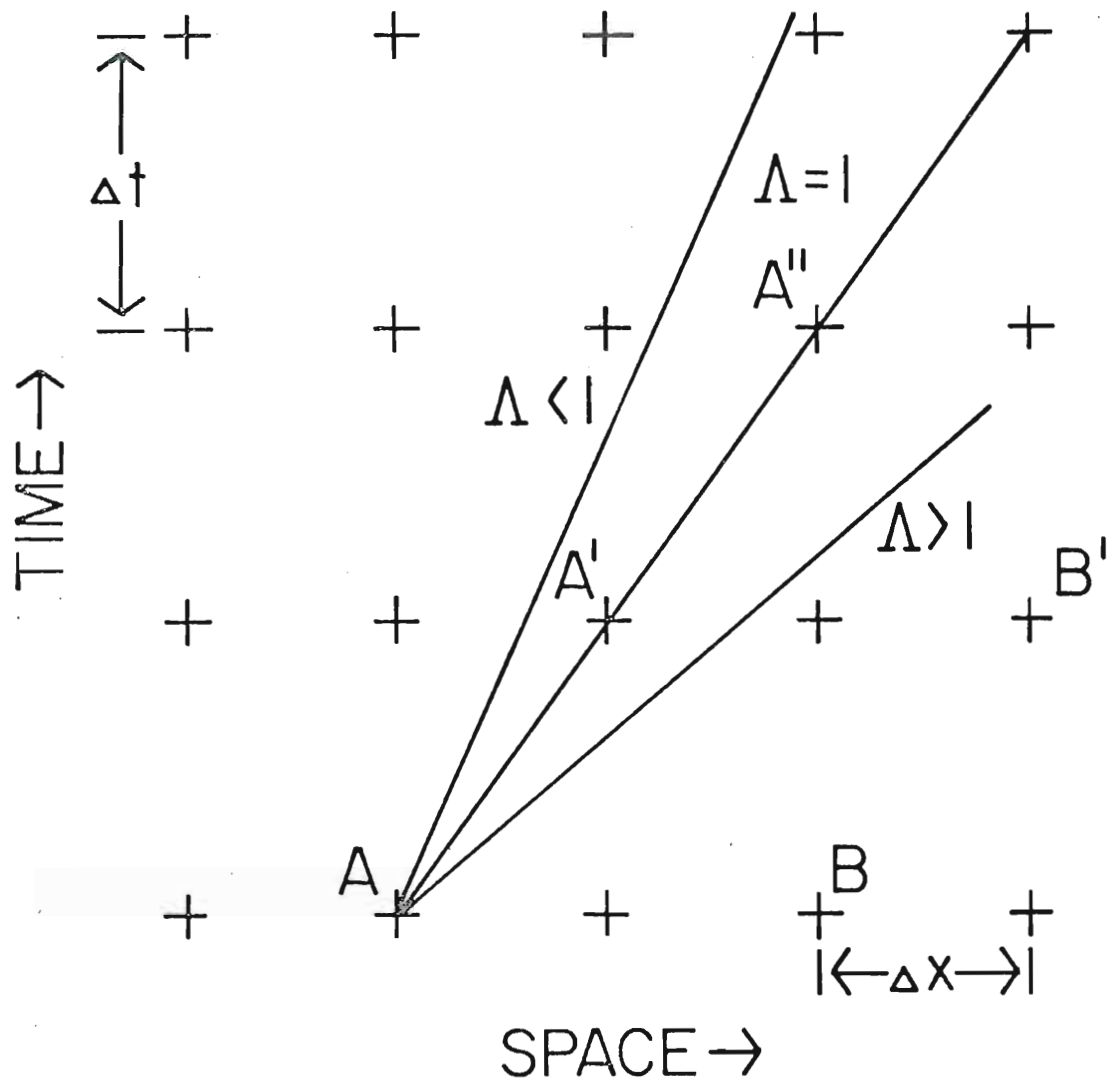


Fig. 4. Three characteristic curves originating from the point A, superimposed on a grid point lattice. The $\Delta < 1$ curve is stable, the $\Delta > 1$ curve is linearly unstable for an explicit formulation. For the explicit formulation used, the characteristic $\Delta = 1$ is predicted from the point A, superimposed on a grid point lattice. The $\Delta < 1$ curve is stable, the $\Delta > 1$ curve is linearly unstable for an explicit formulation. For the explicit formulation used, the characteristic $\Delta = 1$ is predicted exactly.

by slowing down the phase speeds. The rate of slowing down is not uniform. Figure 5 compares the velocities of the waves at various values of Λ to a quantity which will be termed the "CFL velocity"

$$C_{FL} = \frac{\pi \Delta x}{2 \Delta t k \Delta x}$$

If the velocity of any wavenumber exceeds this quantity, then the CFL condition is violated by that wave. We see that at $\Lambda = 1$ all the phase speeds are well below the CFL velocity, and that this velocity is only asymptotically approached for large Λ .

The group velocities for the one-dimensional case $l = 0$ are given by

$$C_{gA} = \frac{d\omega_A}{dk} = U \quad (20)$$

for the analytical, for the explicit

$$C_{gE} = \frac{d\omega_E}{dk} = U \frac{\cos k\Delta x}{(1 - (U \frac{\Delta t}{\Delta x} \sin k\Delta x)^2)^{1/2}} \quad (21)$$

and for the implicit,

$$C_{gI} = \frac{d\omega_I}{dk} = U \frac{\cos k\Delta x}{1 + (U \frac{\Delta t}{\Delta x} \sin k\Delta x)^2} \quad (22)$$

The relations (21) and (22), normalized by (20) are plotted in Fig. 6 for various values of Λ . The dispersive property introduced by the finite differencing has important effects upon the transport of energy. The group velocity for the

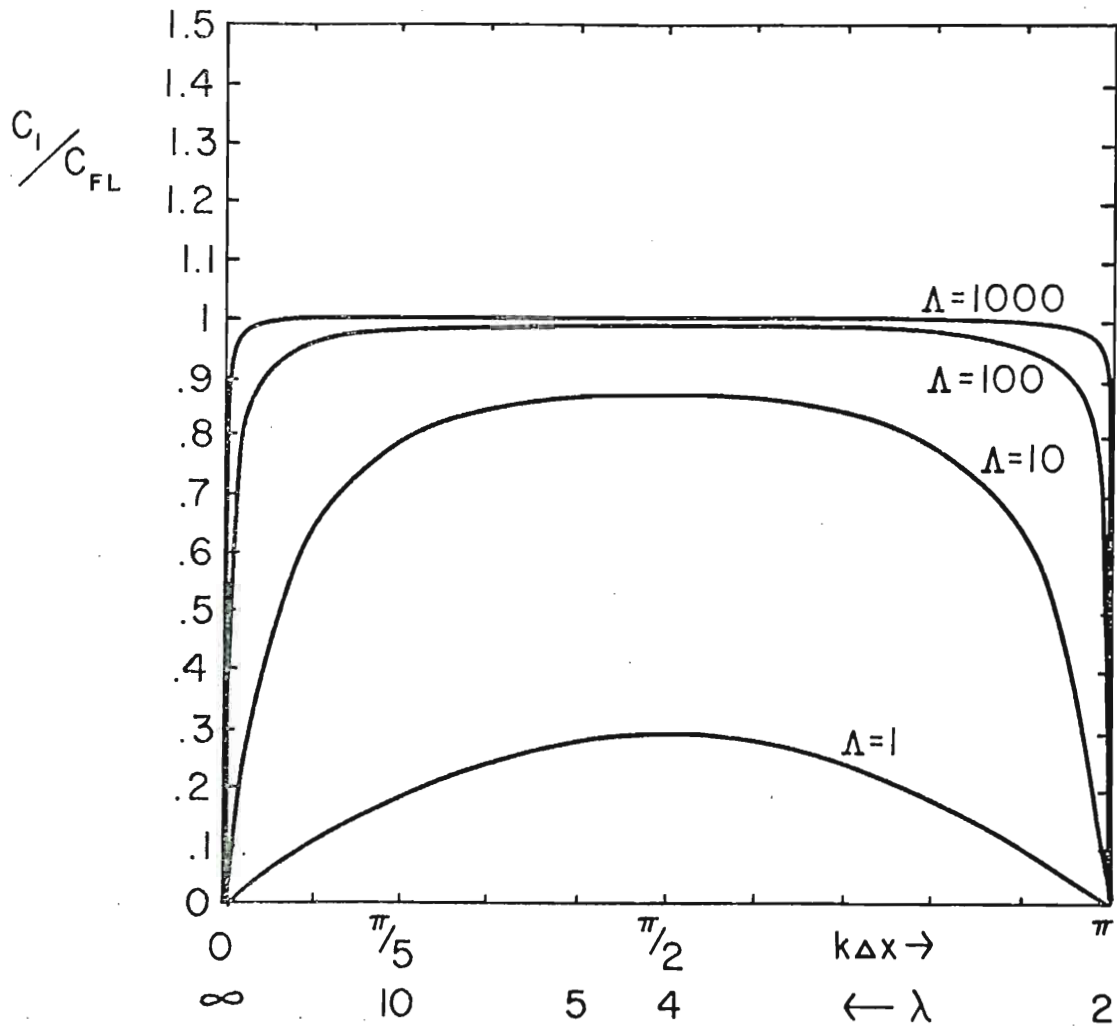


Fig. 5. Comparison of the phase velocity for the implicit formulation to the largest possible phase velocity for stability as a function of wavenumber for various values of Λ . The implicit scheme slows the waves down more than would be required to maintain stability, the limit is only asymptotically approached.

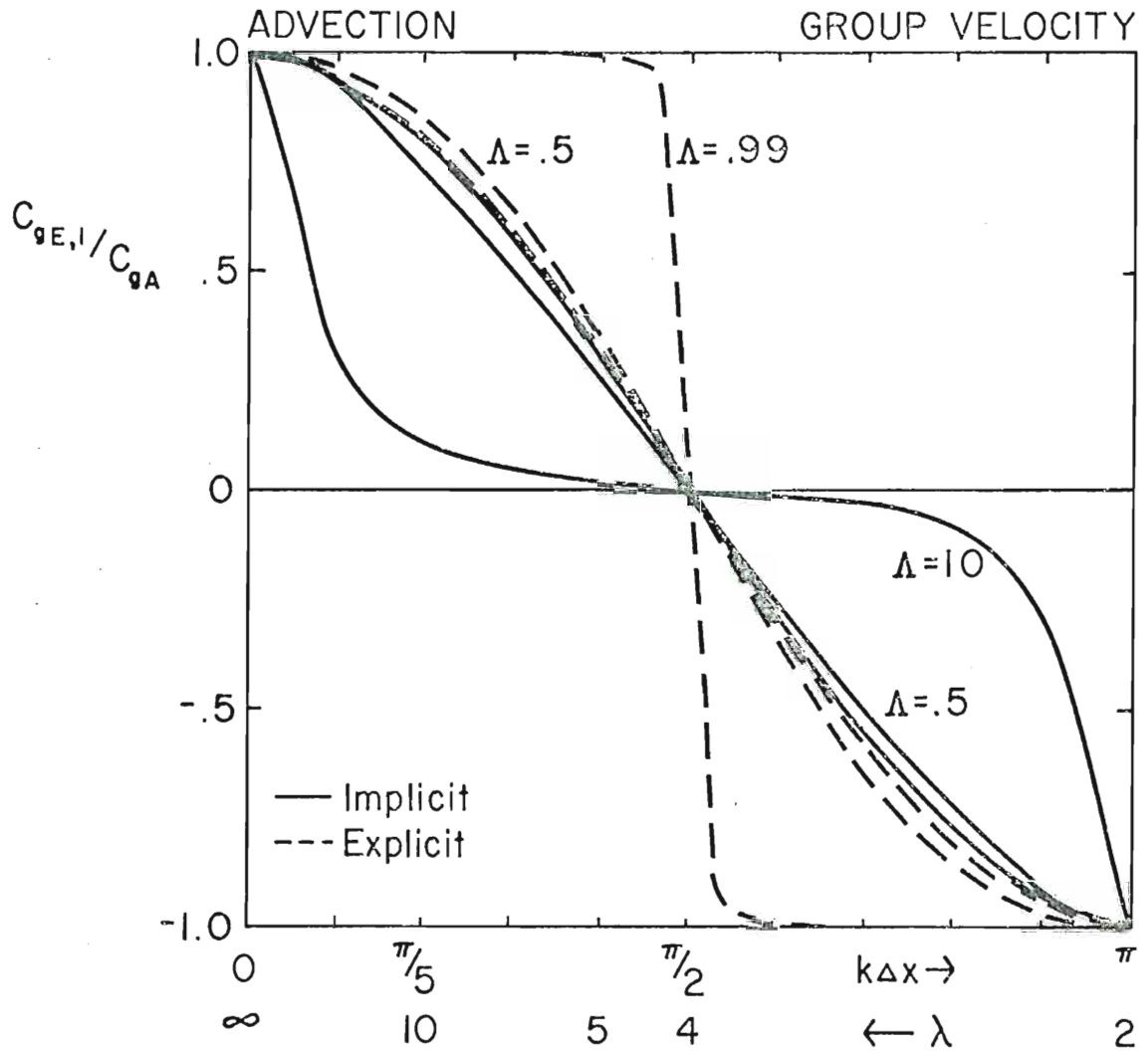


Fig. 6. Group velocities for the one-dimensional advection equation. Velocities of the two numerical schemes are normalized by the analytical value. The explicit scheme is always more accurate than the implicit for waves longer than $4\Delta x$. For waves shorter than $4\Delta x$, the energy in those wavelengths is propagated by both schemes in the opposite direction to the correct group velocity. The explicit scheme is always more accurate than the implicit for waves longer than $4\Delta x$. For waves shorter than $4\Delta x$, the energy in those wavelengths is propagated by both schemes in the opposite direction to the correct group velocity.

long waves ($\gg 4\Delta x$) is approximated reasonably well. The dramatic effect is that energy in waves shorter than $4\Delta x$ is propagated in the opposite direction to the correct velocity. Waves $4\Delta x$ long have zero group velocity. The implicit scheme, for large (typical) values of Λ does a poor job even for the long waves. It is also apparent that the explicit formulation, for low wavenumbers, is always more accurate than the implicit scheme. Finally, Fig. 7 compares the explicit version of the second order scheme to the fourth order scheme. Where the group velocity for the latter is given by

$$U \left[\frac{\frac{4}{3} \cos k\Delta x - \frac{1}{3} \cos 2k\Delta x}{\left(1 - \left(\frac{4}{3} U \frac{\Delta t}{\Delta x} \sin k\Delta x - U \frac{\Delta t}{6\Delta x} \sin 2k\Delta x\right)^2\right)^{1/2}} \right]$$

The fourth order scheme actually does worse than the second order for the shortest waves. However, the long waves are handled quite well, though their phase speed is overestimated.

Gravity waves can be modelled by the following set of equations

$$u_t = -\phi_x \quad v_t = -\phi_y \quad \phi_t + \phi(u_x + v_y) = 0$$

where ϕ is a mean state geopotential. A dispersion relation can be obtained using solutions for u , v and ϕ of the form

(15)

$$\omega_A = \pm (\phi (k^2 + \ell^2))^{1/2} \quad (23)$$

An explicit formulation

$$\omega_A = \pm (\psi (k^2 + \ell^2)) \quad (24)$$

An explicit formulation

$$u^{n+1} = u^{n-1} - \frac{\Delta t}{\Delta x} (\phi_{j+1}^n - \phi_{j-1}^n)$$

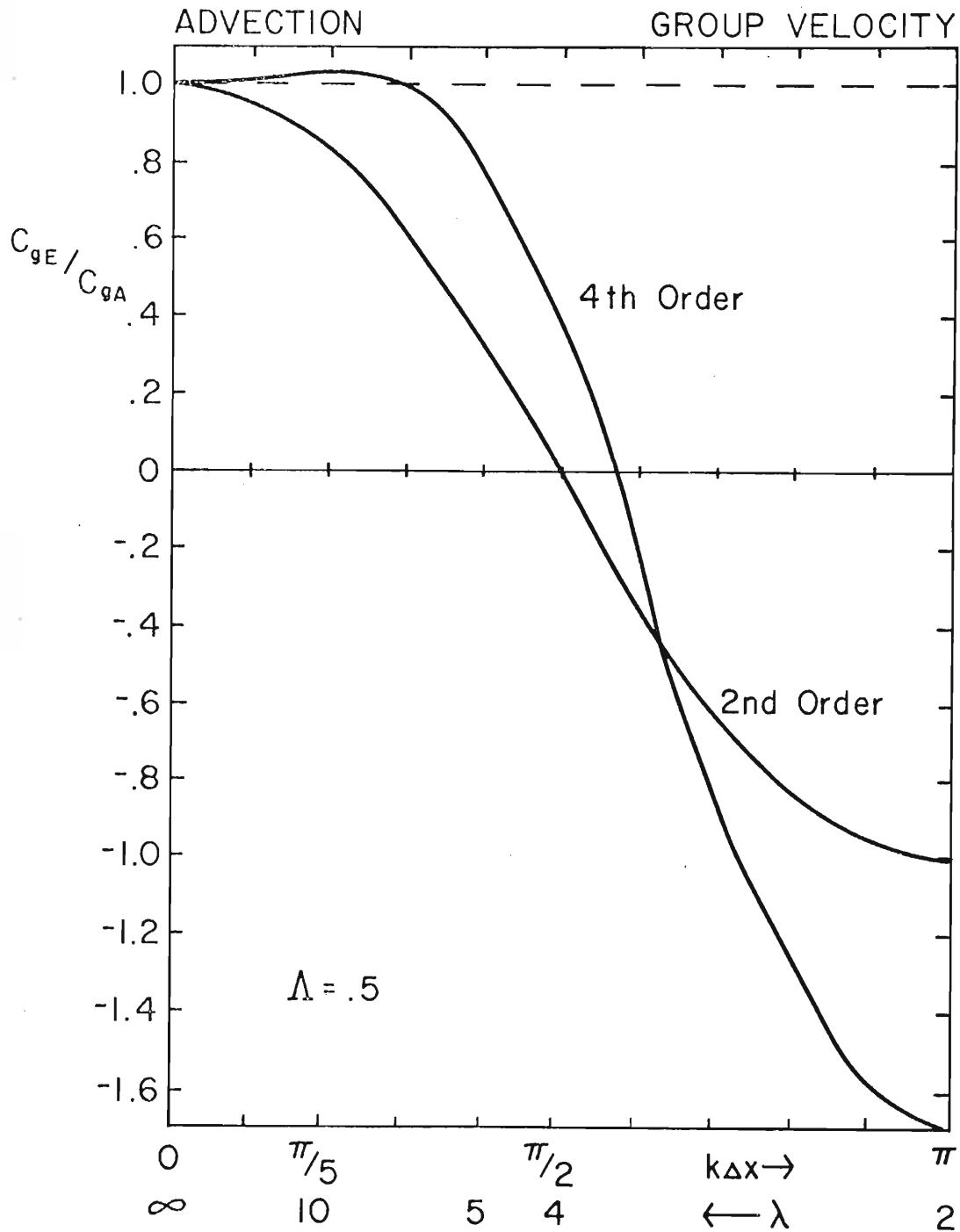


Fig. 7. Comparison of the group velocities between a so-called "fourth order" scheme and the "second order", centered-in-space scheme as a function of wavenumber.

Long waves are treated quite well by the higher order scheme. Fig. 7. Comparison of the group velocities between a so-called "fourth order" scheme and the "second order", centered-in-space scheme as a function of wavenumber. Long waves are treated quite well by the higher order scheme, however its treatment of the shortest waves is inferior to the second order scheme.

$$v^{n+1} = v^{n-1} - \frac{\Delta t}{\Delta y} (\phi_{m+1}^n - \phi_{m-1}^n)$$

$$\phi^{n+1} = \phi^{n-1} - \phi \left[\frac{\Delta t}{\Delta x} (u_{j+1}^n - u_{j-1}^n) + \frac{\Delta t}{\Delta y} (v_{m+1}^n - v_{m-1}^n) \right]$$

after substitution of solutions of the form (17) implies that

$$\omega_E = \frac{1}{\Delta t} \arcsin \left\{ \pm \left[\phi \Delta t^2 \left(\frac{\sin^2 k \Delta x}{\Delta x^2} + \frac{\sin^2 \ell \Delta y}{\Delta y^2} \right) \right]^{1/2} \right\} \quad (24)$$

An implicit formulation

$$u^{n+1} = u^n - \frac{\Delta t}{4\Delta x} \left(\phi_{j+1}^n + \phi_{j+1}^{n+1} - \phi_{j-1}^n - \phi_{j-1}^{n+1} \right)$$

$$v^{n+1} = v^n - \frac{\Delta t}{4\Delta y} \left(\phi_{m+1}^n + \phi_{m+1}^{n+1} - \phi_{m-1}^n - \phi_{m-1}^{n+1} \right)$$

$$\begin{aligned} \phi^{n+1} = \phi^n - \phi \left[\frac{\Delta t}{4\Delta x} (u_{j+1}^n + u_{j+1}^{n+1} - u_{j-1}^n - u_{j-1}^{n+1}) \right. \\ \left. + \frac{\Delta t}{4\Delta y} (v_{m+1}^n + v_{m+1}^{n+1} - v_{m-1}^n - v_{m-1}^{n+1}) \right] \end{aligned}$$

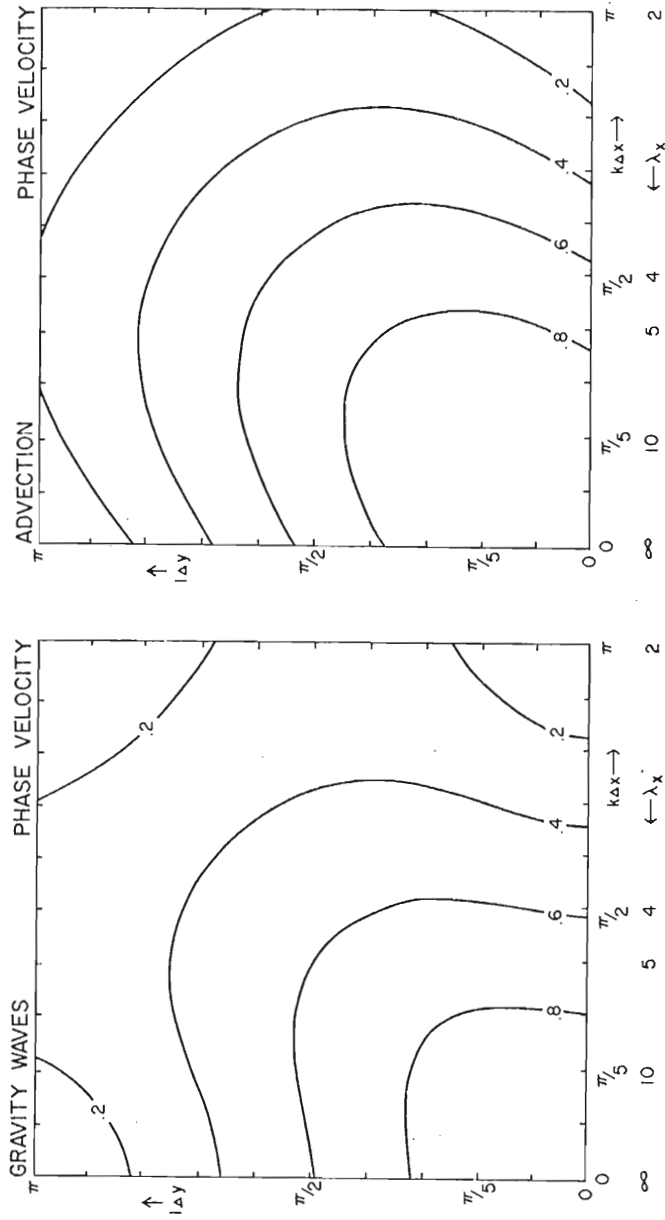
yields in a similar fashion

$$\omega_I = \frac{2}{\Delta t} \arctan \left\{ \pm \left[\phi \frac{\Delta t^2}{4} \left(\frac{\sin^2 k \Delta x}{\Delta x^2} + \frac{\sin^2 \ell \Delta y}{\Delta y^2} \right) \right]^{1/2} \right\} \quad (25)$$

Because of the symmetry of the relations (23)-(25) we need consider only the one-dimensional case $\ell = 0$. The solutions behave quite similarly to the case of the one-dimensional advection equation; both are shown in Fig. 8.

The components of the vector group velocities are symmetric so we will consider only one of them. Here,

The components of the vector group velocities are symmetric so we will consider only one of them. Here, however, ℓ will be treated as a parameter and allowed to vary instead of setting it to zero. The true group



(a)

(b)

Fig. 8. Contour plots of the phase frequency for the two-dimensional (a) gravity waves system and (b) advection equation. The frequencies are normalized by the analytical solutions for various values of the x and y wavenumbers, k and l .

velocity is

$$C_{gA} = \frac{\pm \phi^{1/2} k}{(k^2 + \ell^2)^{1/2}} \quad (26)$$

The explicit version is

$$C_{gE} = \frac{\pm \phi^{1/2} \sin k\Delta x \cos k\Delta x}{\Delta x (1 - \Delta t^2 A)^{1/2} A^{1/2}} \quad (27)$$

where

$$A = \frac{\sin^2 k\Delta x}{\Delta x^2} + \frac{\sin^2 \ell\Delta y}{\Delta y^2}$$

and the implicit version is

$$C_{gI} = \pm \frac{\phi^{1/2} \sin k\Delta x \cos k\Delta x}{\Delta x \left[1 + \phi \frac{\Delta t^2}{4} A \right] A^{1/2}} \quad (28)$$

Contour plots of these relations appear in Figs. 9 and 10. Figure 9 compares the explicit formulation (27) to the analytical, (26), for a $\Lambda = \phi \Delta t^2 / \Delta x^2$ ratio near the maximum allowable for stability ($\Delta x = \Delta y$ for simplicity here). A graph of the implicit formulation for the same value of Λ is very similar to Fig. 9, and is not reproduced, instead a plot is presented for a value of Λ considerably in excess of that used in Fig. 9.

The solutions to the governing equations are plane waves and relations (26)-(28) are merely the component of the group velocity in the x direction. There will be errors in the direction of the vector group velocity as well as in the group velocity in the x direction. There will be errors in the direction of the vector group velocity as well as in the magnitude. In some cases these errors can be quite large, particularly for waves which are traveling nearly

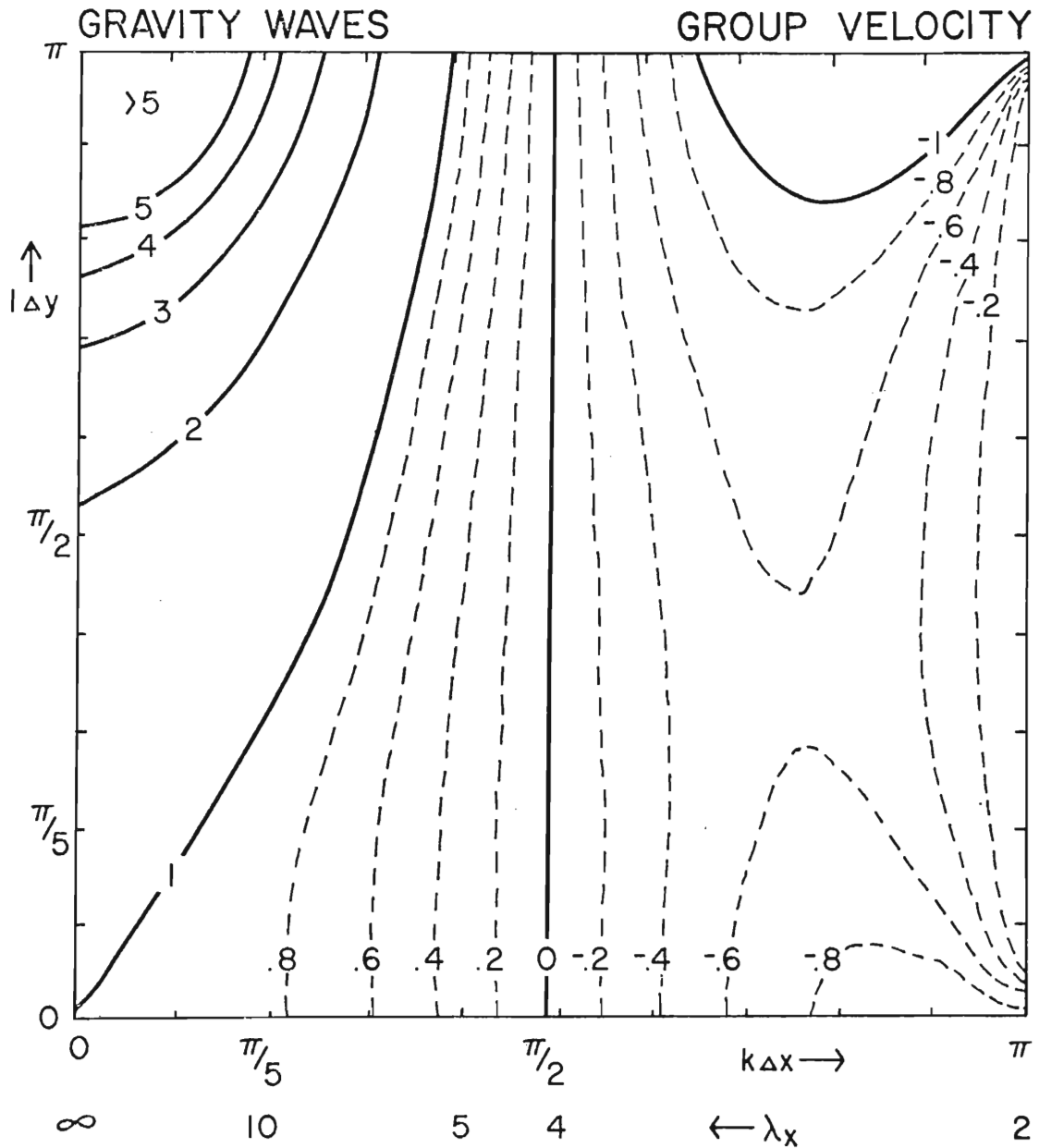


Fig. 9. x component of the vector group velocity of the gravity waves for the explicit scheme, at $\Lambda = 0.5$. The contours are normalized by the correct group velocity.

the gravity waves for the explicit scheme, at $\Lambda = 0.5$. The contours are normalized by the correct group velocity.

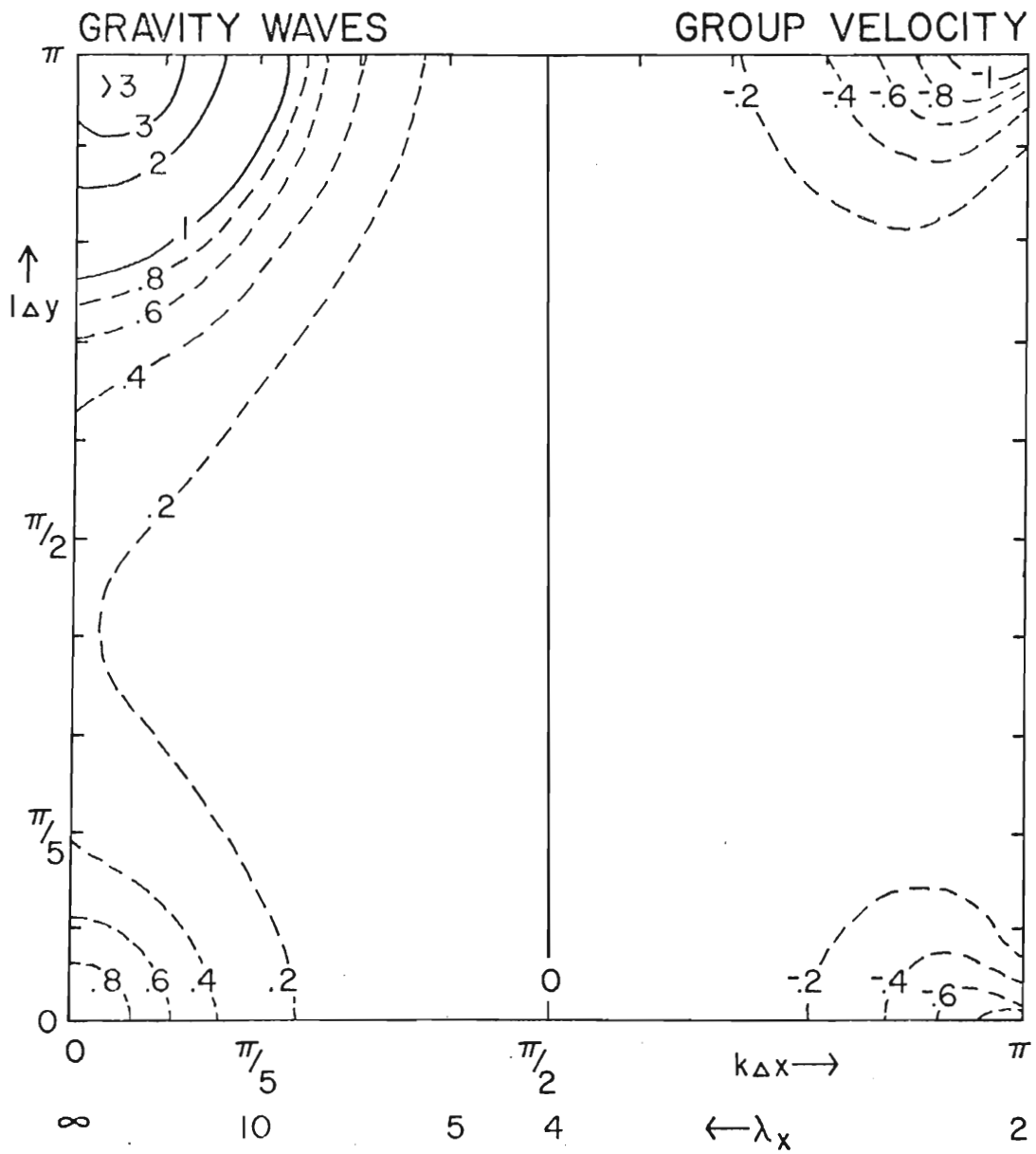
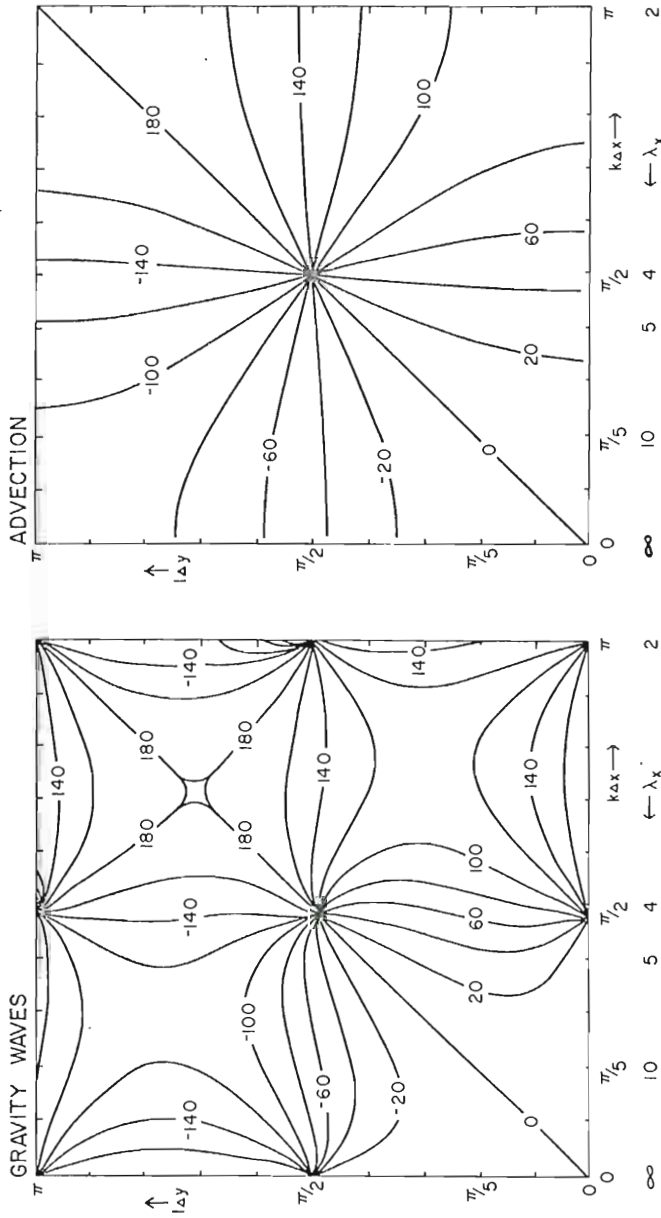


Fig. 10. Same as Fig. 9 except for the implicit scheme for $\Lambda = 10$.

Fig. 10. Same as Fig. 9 except for the implicit scheme for $\Lambda = 10$.

perpendicular to the direction of the derivative. Figure 11 is a contour plot of the angular error in the group velocity for the gravity waves and for the two-dimensional advection solution. The lines are of constant angle measured positive counterclockwise from the correct angle (note that a 180° error is equivalent to a -180° error). This error is the same for all values of Δt and Δx , and for the implicit and explicit schemes. The contours do not intersect the axis for the advection plot since the problem becomes one-dimensional and thus the angular error is either 0 or 180° .



(a)

(b)

Fig. 11. Contour plots of the angular error in the vector group velocity of the numerical schemes measured counterclockwise from the correct direction for the two-dimensional (a) gravity waves system and (b) advection equation. Lines in (b) do not intersect the axes since the problem changes character there.

4. COMPLEX SYSTEMS

In the previous section we considered three simple systems, each with one distinct mode. More typical problems with more than one mode and non-constant coefficients will now be considered. The explicit and implicit formulations will be combined into a semi-implicit approach for some of the analysis.

The full shallow water primitive equations on an f-plane are

$$\begin{aligned}u_t + Uu_x + Vu_y &= f_0 v - \phi_x \\v_t + Uv_x + Vv_y &= -f_0 u - \phi_y \\ \phi_t + U\phi_x + V\phi_y + \Phi(u_x + v_y) &= 0\end{aligned}\tag{29}$$

where f_0 is a constant Coriolis parameter. Assuming solutions for u , v and ϕ of the form (15) one can show that there are three phase frequencies given by

$$\begin{aligned}\omega_A &= Uk + V\ell \\ \omega_A &= Uk + V\ell \pm (f_0^2 + \Phi(k^2 + \ell^2))^{1/2}\end{aligned}\tag{30}$$

These are merely the advection solution and two inertia-gravity waves doppler shifted by the mean state velocity.

A simple semi-implicit scheme for (29) is gravity waves doppler shifted by the mean state velocity.

A simple semi-implicit scheme for (29) is

$$\begin{aligned}
u^{n+1} &= u^{n-1} - U \frac{\Delta t}{\Delta x} \left(u_{j+1}^n - u_{j-1}^n \right) - V \frac{\Delta t}{\Delta y} \left(v_{m+1}^n - v_{m-1}^n \right) \\
&\quad + 2\Delta t f_0 v^n - \frac{\Delta t}{2\Delta t} \left(\phi_{j+1}^{n+1} + \phi_{j+1}^{n-1} - \phi_{j-1}^{n+1} - \phi_{j-1}^{n-1} \right) \\
v^{n+1} &= v^{n-1} - U \frac{\Delta t}{\Delta x} \left(v_{j+1}^n - v_{j-1}^n \right) - V \frac{\Delta t}{\Delta y} \left(v_{m+1}^n - v_{m-1}^n \right) \\
&\quad - 2\Delta t f_0 u^n - \frac{\Delta t}{2\Delta y} \left(\phi_{m+1}^{n+1} + \phi_{m+1}^{n-1} - \phi_{m-1}^{n+1} - \phi_{m-1}^{n-1} \right) \\
\phi^{n+1} &= \phi^{n-1} - U \frac{\Delta t}{\Delta x} \left(\phi_{j+1}^n - \phi_{j-1}^n \right) - V \frac{\Delta t}{\Delta y} \left(\phi_{m+1}^n - \phi_{m-1}^n \right) \\
&\quad - \phi \frac{\Delta t}{2\Delta x} \left(u_{j+1}^{n+1} + u_{j+1}^{n-1} - u_{j-1}^{n+1} - u_{j-1}^{n-1} \right) \\
&\quad - \phi \frac{\Delta t}{2\Delta y} \left(v_{m+1}^{n+1} + v_{m+1}^{n-1} - v_{m-1}^{n+1} - v_{m-1}^{n-1} \right) \tag{31}
\end{aligned}$$

Now, substitute solutions of the form (17) into (31). After considerable algebraic manipulation, the two roots corresponding to the inertia-gravity waves (30) are

$$\omega_{SI} = \frac{1}{\Delta t} \arcsin \left\{ \left[\pm R^{1/2} + A \right] / P \right\} \tag{32}$$

where

$$\begin{aligned}
A &= U \frac{\Delta t}{\Delta x} \sin k\Delta x + V \frac{\Delta t}{\Delta y} \sin \ell\Delta y \\
P &= \phi \Delta t^2 \left[\frac{\sin^2 k\Delta x}{\Delta x^2} + \frac{\sin^2 \ell\Delta y}{\Delta y^2} \right] + 1 \\
R &= \left[\Delta t^2 f_0^2 - 1 - A^2 \right] / P + P^2 + A^2
\end{aligned}$$

The advection root of this finite differenced set is merely Eq. (18). However, the eigenvector for this set will be different from that for the explicit version of (14). Equation (18). However, the eigenvector for this set will be different from that for the explicit version of (14). Equation (32) is compared with (30) in Fig. 12. The nature of the variation appears suspiciously similar to a pure

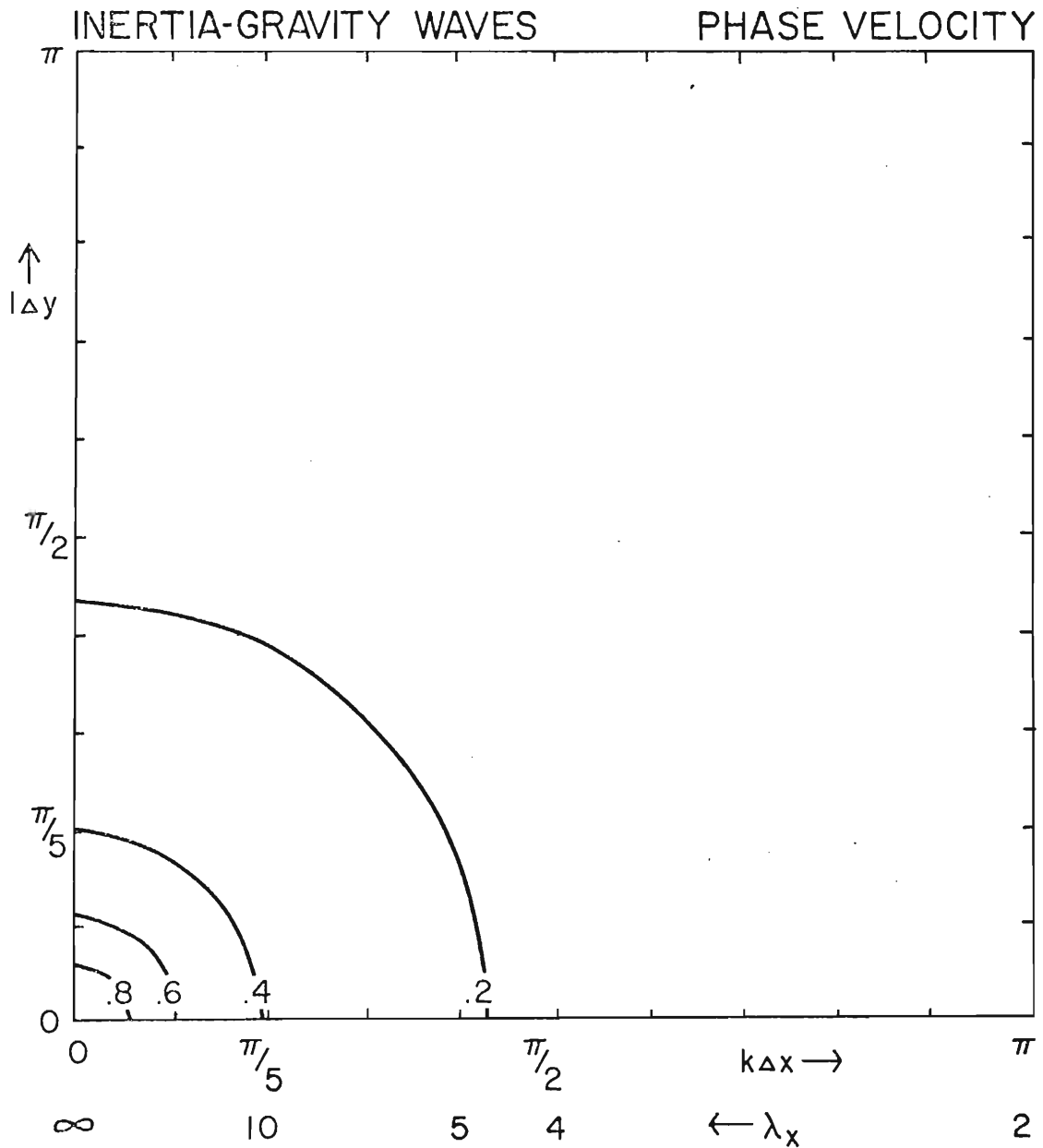


Fig. 12. Contours of the phase frequency of the inertia-gravity waves in the semi-implicit scheme normalized by the analytical frequency for $\Lambda = 0.5$. This figure is consistent with the results from the gravity wave system treated in Section 3.

by the analytical frequency, consistent with the results from the gravity wave system treated in Section 3.

implicit treatment of gravity waves; indeed, that is essentially what takes place. The advection or "quasi-geostrophic" modes were compared in Section 3. In this linear problem, the mixture of the time schemes for different modes affects those modes essentially individually.

The group velocity components are again symmetric; the x component is given by

$$C_{gA} = U \pm \phi k \left(f_0^2 + \phi(k^2 + l^2) \right)^{-1/2}$$

for the analytical, and for the semi-implicit:

$$C_{gSI} = \frac{1}{\Delta t} \left(1 - \left\{ [\pm R^{1/2} + A]/P \right\}^2 \right)^{-1/2} \frac{dB}{dk}$$

where

$$\frac{dB}{dk} = \frac{-(\pm R^{1/2} + A)}{P^2} \frac{dP}{dk} + P^{-1} \left\{ \pm \frac{1}{2} R^{-1/2} \frac{dR}{dk} + \frac{dA}{dk} \right\}$$

$$\frac{dA}{dk} = U \Delta t \cos k \Delta x$$

$$\frac{dP}{dk} = 2\phi \frac{\Delta t^2}{\Delta x} \cos k \Delta x \sin k \Delta x$$

$$\frac{dR}{dk} = [\Delta t^2 f_0^2 - 1 - A^2] \frac{d\phi}{dk} - 2AP \frac{dA}{dk} + 2P \frac{dP}{dk} + 2A \frac{dA}{dk}$$

One sees in Fig. 13, that near the stability limit, determined mainly by the advection speed, the inertia-gravity waves are transporting their energy far below the correct speed. This is consistent with the results of one-dimensional gravity waves presented in Fig. 7 for an implicit speed. This is consistent with the results of one-dimensional gravity waves presented in Fig. 7 for an implicit treatment at high values of Λ .

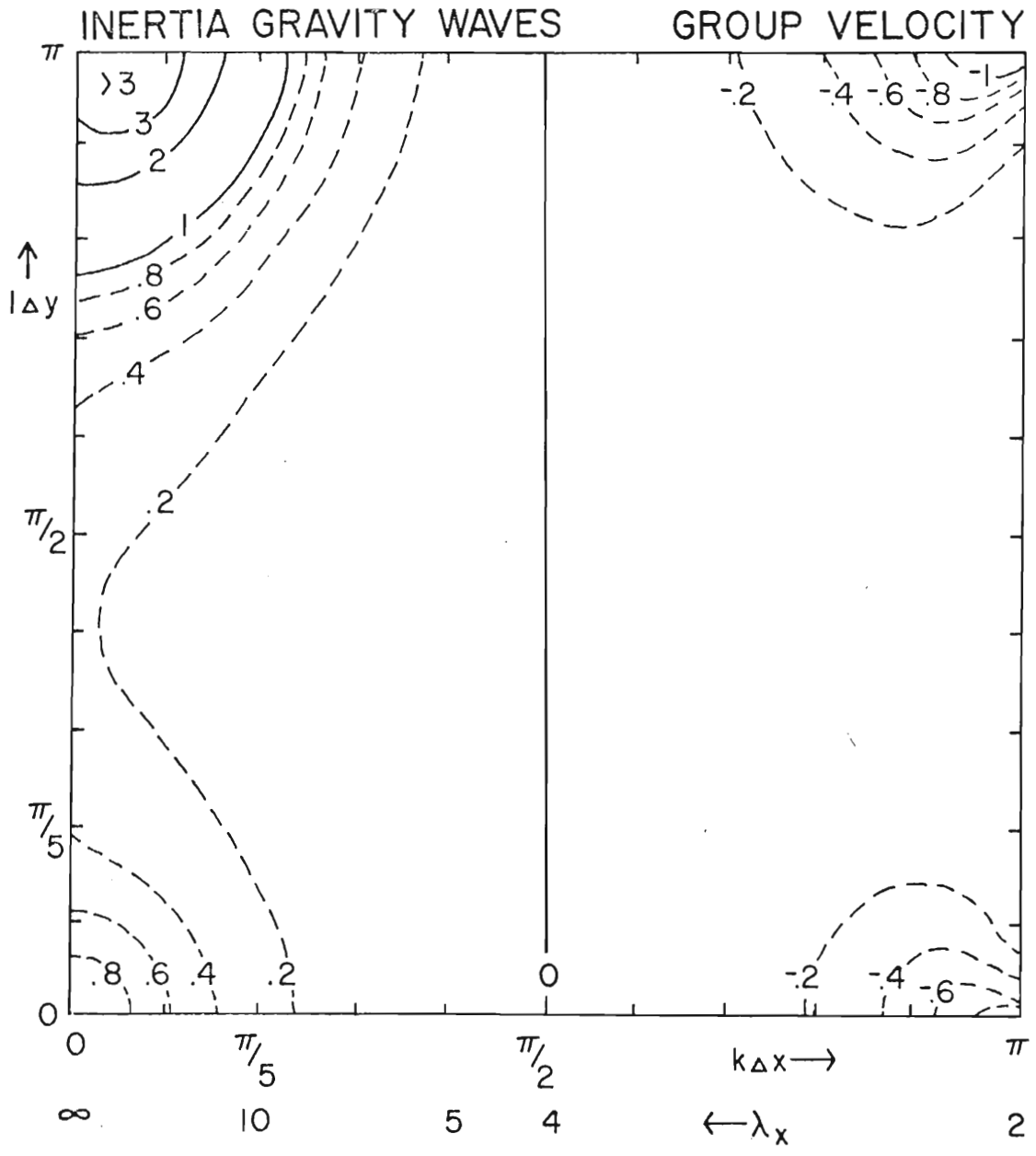


Fig. 13. x component of the vector group velocity of the semi-implicit case normalized by the correct value for $\Lambda \sim 10$. Note similarity to the pure gravity wave case presented in Fig. 10.

$\Lambda \sim 10$. Note similarity to the pure gravity wave case presented in Fig. 10.

Results similar to those from the f-plane primitive equations are obtained for a semi-implicit two-layer set. The internal gravity waves are handled like slow moving gravity waves, the external gravity waves are handled as in the previous case. The treatment of the different components of the modes, either explicitly or implicitly, again separates out. This is in part a consequence of the CFL condition being exceeded (that is Δ large) only for the external gravity waves, so that the explicit and implicit treatments of the other modes are nearly equivalent. It is therefore reasonable to infer that the mixture of time schemes when the modes are widely separated, affects those modes essentially individually. Since semi-implicit schemes are used when one has waves which move much faster than others, the behavior of either set of waves can be closely approximated by an implicit or explicit treatment of the whole model. This is not too surprising for a linear model and is fortunate, since the analytical derivation of the semi-implicit phase frequencies can be intractable when either an explicit or implicit scheme is solvable.

The quasi-geostrophic mode is generally of more interest than inertia-gravity waves for the atmosphere since it contains the major part of the energy in the large-scale mid-latitude flows. However, inertia-gravity waves are of major interest in oceanography, both for tidal problems and on a smaller scale for internal waves. The very

small inertia-gravity waves are generally of less interest. The inertia-gravity waves are the apparent mechanism for bringing the flow and pressure fields into geostrophic balance for both the atmosphere and ocean (e.g., Blumen, 1972). Thus, errors in their estimation may affect the adjustment time scales of numerical models.

Next we will introduce a variable Coriolis parameter, f , by considering the nondivergent barotropic vorticity equation. This model was commonly used for large-scale atmospheric prediction, until more sophisticated, primitive equation models were developed. However, it remains an important tool for representing many important dynamic processes. Gates has studied the errors caused by numerical integration of a one-dimensional form of this equation. The results to be presented here for phase speeds are consistent with his analytical studies (Gates, 1959) and comparisons of actual integrations with known harmonic solutions (Gates and Riegel, 1962).

If we define a streamfunction ψ :

$$v = \frac{\partial \psi}{\partial x}, \quad u = -\frac{\partial \psi}{\partial y}$$

then our vorticity equation, for two dimensions, can be written

$$\frac{\partial}{\partial t} \nabla^2 \psi + \beta \frac{\partial \psi}{\partial x} = 0 \quad (33)$$

where ∇^2 is the horizontal Laplacian operator, and $\beta = df/dy$.

where ∇^2 is the horizontal Laplacian operator, and $\beta = df/dy$. Assume that the solution for ψ has the form (15), then (33) yields a dispersion relation

$$\omega_A = \frac{-\beta k}{k^2 + \ell^2} \quad (34)$$

If we finite difference (33) in the following explicit manner, using a five point, "second order" Laplacian operator

$$\begin{aligned} & \frac{1}{\Delta x^2} \left(\psi_{j+1}^{n+1} + \psi_{j-1}^{n+1} - 2\psi_j^{n+1} \right) + \frac{1}{\Delta y^2} \left(\psi_{m+1}^{n+1} + \psi_{m-1}^{n+1} - 2\psi_m^{n+1} \right) = \\ & \frac{1}{\Delta x^2} \left(\psi_{j+1}^{n-1} + \psi_{j-1}^{n-1} - 2\psi_j^{n-1} \right) + \frac{1}{\Delta y^2} \left(\psi_{m+1}^{n-1} + \psi_{m-1}^{n-1} - 2\psi_m^{n-1} \right) - \\ & - \frac{\Delta t \beta}{\Delta x} \left(\psi_{j+1}^n - \psi_{j-1}^n \right) \end{aligned}$$

the corresponding phase frequency is obtained

$$\omega_E = \frac{1}{\Delta t} \arcsin \left\{ \frac{-\beta \Delta t \sin k \Delta x}{4 \Delta x A} \right\}$$

where

$$A = \frac{\sin^2 \left(\frac{k \Delta x}{2} \right)}{\Delta x^2} + \frac{\sin^2 \left(\frac{\ell \Delta y}{2} \right)}{\Delta y^2}$$

An implicit scheme, where all the terms are at the n and $n+1$ time levels dictates a phase frequency satisfying

$$\omega_I = \frac{2}{\Delta t} \arctan \left\{ \frac{-\beta \Delta t \sin k \Delta x}{8 \Delta x A} \right\}$$

In a typical problem where Rossby waves are being studied, there will be other modes which may require a much lower ratio of $\Delta t/\Delta x$ for stability than that for pure Rossby waves. Therefore a value of $\Delta t/\Delta x = 10^{-1}$ s m⁻¹ was chosen. Since β is so small (around 10^{-11} m⁻¹ s⁻¹ for the earth) and the arctangent of a small number approximates the arcsine of that number, then the two treatments are essentially identical. The arctangent of a small number approximates the arcsine of that number, then the two treatments are essentially identical. The phase velocity of the finite differenced equations

is compared with the continuous solution (34) in Fig. 14. When the motion is generally directed more in the x direction, the numerical schemes underestimate the phase speed. When the motion is mostly in the y direction the velocity is overestimated for small k.

The components of the group velocity here are not symmetric; consider the x component first. The analytical and numerical components are, respectively

$$C_{gAx} = \beta \left[\frac{k^2 - \ell^2}{(k^2 + \ell^2)^2} \right]$$

$$C_{gNx} \approx \frac{\beta}{4} \left[\frac{\sin k\Delta x \sin \frac{k\Delta x}{2} \cos \frac{k\Delta x}{2}}{\Delta x^2 A^2} - \frac{\cos k\Delta x}{A} \right]$$

The x component is generally overestimated by the numerical scheme, particularly for large values of k and ℓ . Note that the energy in waves which propagate at a 45° angle will have a nonzero x component in the numerical scheme. In contrast, the y component is handled reasonably well. The y component functions of the group velocity are

$$C_{gAy} = \frac{2\beta\ell k}{(k^2 + \ell^2)^2}$$

and

$$C_{gNy} \approx \frac{\beta}{4\Delta x} \left[\frac{\sin k\Delta x \sin \frac{\ell\Delta y}{2} \cos \frac{\ell\Delta y}{2}}{\Delta y A^2} \right]$$

for the analytical and numerical models. Again there will be significant errors in the direction as well as the magnitude for the analytical and numerical models. Again there will be significant errors in the direction as well as the magnitude of the group velocity in the numerical model. These

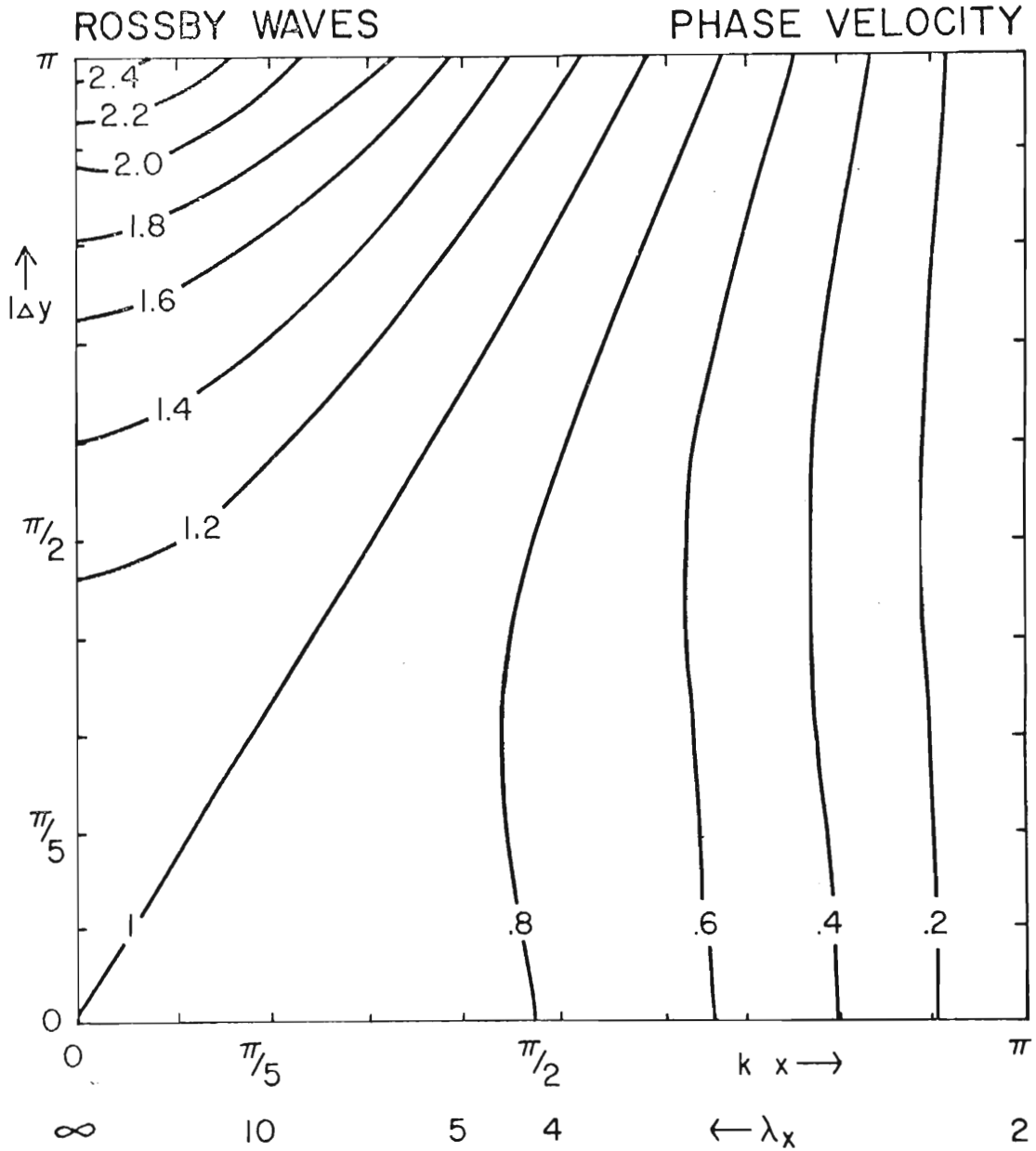


Fig. 14. Phase velocity for the numerical treatment of the nondivergent barotropic vorticity equation normalized by the correct velocity of the Rossby waves.

Fig. 14. Phase velocity for the numerical treatment of the nondivergent barotropic vorticity equation normalized by the correct velocity of the Rossby waves.

are illustrated in Figs. 15 and 16, respectively.

The final case examined will be the primitive equations on an equatorial β -plane. Our governing equations are a special case of Laplace's tidal equations (LTE):

$$\begin{aligned} u_t + Uu_x &= \beta y v - \phi_x \\ v_t + Uv_y &= -\beta y u - \phi_y \\ \phi_t + U\phi_x + \Phi(u_x + v_y) &= 0 \end{aligned} \quad (35)$$

This and similar versions of LTE have been extensively studied analytically. Miles (1974) presents an excellent review of the classical tidal problem. The solutions of (35) are contained in Matsuno (1966); they are two waves which behave like gravity waves and a third which is like a Rossby wave. Lindzen (1970) referred to the latter solution as a Rossby-Haurwitz wave. He allowed for vertical propagation in his treatment and also derived an approximate solution for a mid-latitude β -plane.

To solve (35) substitute a solution of the form

$$F(y) e^{i(kx - \omega t)}$$

for u , v and ϕ , where the y dependence, denoted by some function F , is left unspecified. The set of equations is then manipulated into an ordinary differential equation (ODE) in y for v . (The details of this derivation are presented in Appendix 2.)
(ODE) in y for v . (The details of this derivation are presented in Appendix 2.)

$$\frac{d^2 v}{dy^2} + \left(\frac{A^2}{\Phi} - k^2 - \frac{\beta k}{A} - \frac{\beta^2 y^2}{\Phi} \right) v = 0 \quad (36)$$

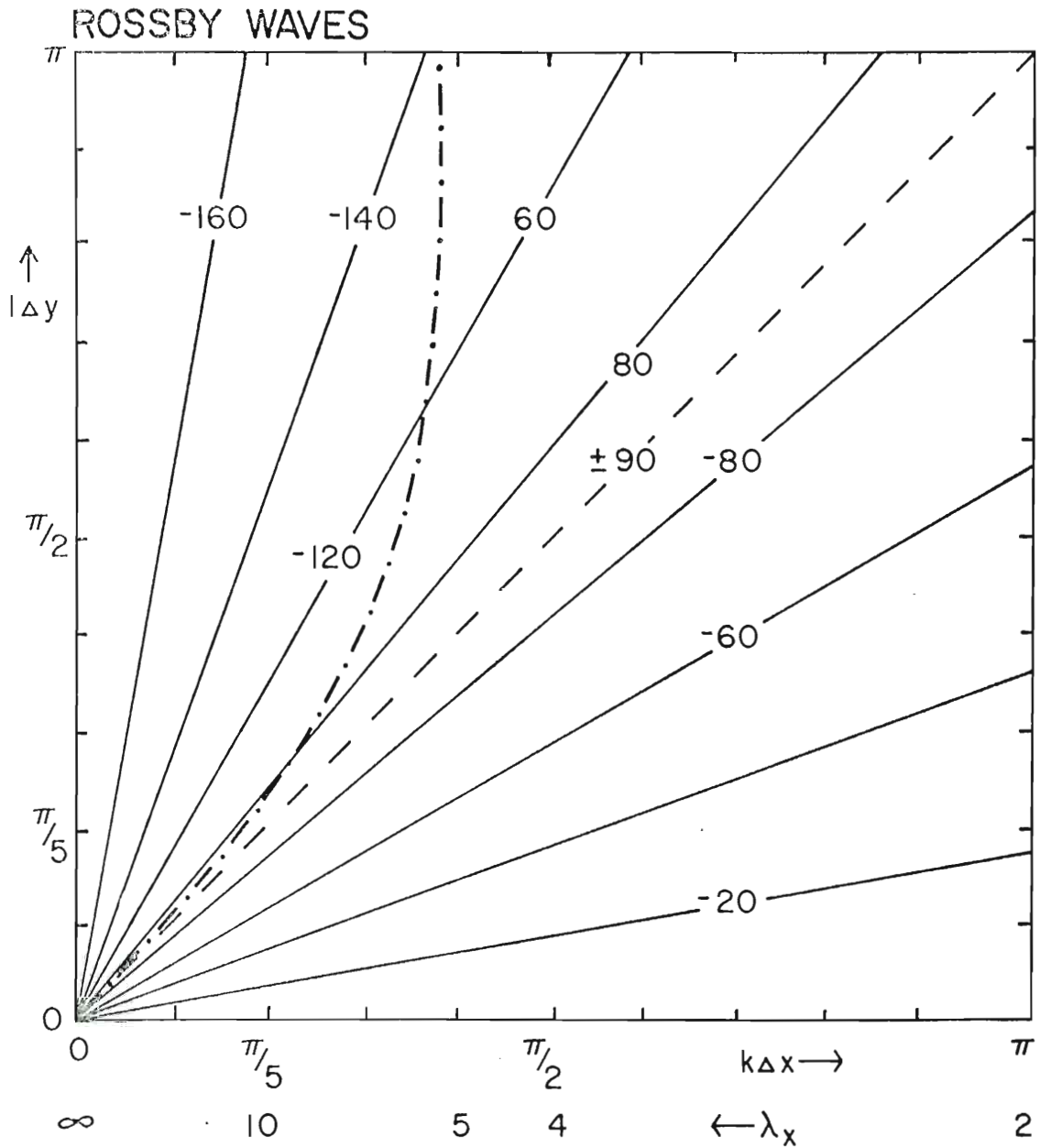


Fig. 15. Contour plot of the directional error in the vector group velocity for the numerical formulations of the vorticity equation. The x components of the correct and numerical group velocities are zero along the dashed and dot-dashed lines, respectively.

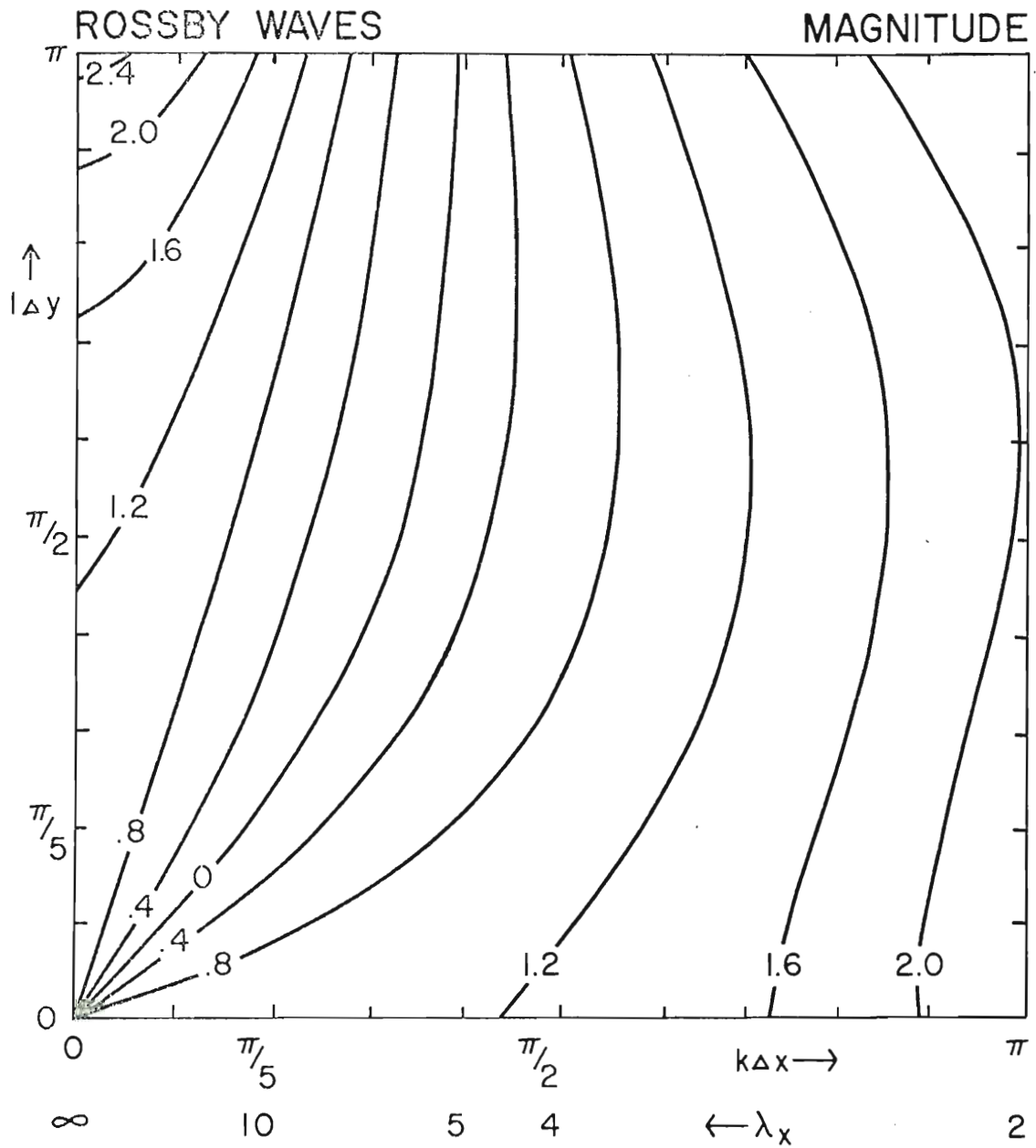


Fig. 16. Plot of the magnitude of the group velocity for the numerical schemes normalized by the correct value.

for the numerical schemes normalized by the correct value.

where

$$A = \omega - Uk$$

The boundary conditions for (36) are $v \rightarrow 0$ as $y \rightarrow \pm \infty$.

Assume that the y dependent part of the solution for v has the form

$$v(y) = G(y) e^{-\frac{1}{2} \frac{\beta}{\Phi} y^2} \quad (37)$$

This will leave the following ODE for G :

$$G'' - \frac{2\beta}{\sqrt{\Phi}} y G' + \left(\frac{A^2}{\Phi} - k^2 - \frac{\beta k}{A} - \frac{\beta^2 y^2}{\Phi} \right) G = 0$$

where primes denote differentiation with respect to y . If we assume a polynomial solution for G :

$$G = \sum_{\eta=0}^{\infty} C_{\eta} y^{\eta}$$

then one obtains the recursion formula

$$C_{\eta+2} = -C_{\eta} \frac{\left(\frac{A^2}{\Phi} - k^2 - \frac{\beta k}{A} - \frac{\beta}{\sqrt{\Phi}} - \frac{2\beta\eta}{\sqrt{\Phi}} \right)}{(\eta+2)(\eta+1)}$$

In order for v to satisfy the boundary conditions, G must be truncated at some value of η . Thus there are an infinite number of modes in the y direction – one for each value of η . They satisfy the dispersion relation

$$A^3 + aA + b = 0 \quad (38)$$

where

$$a = - (k^2 \Phi + (2\eta + 1) \beta \sqrt{\Phi})$$

where

$$a = - (k^2 \Phi + (2\eta + 1) \beta \sqrt{\Phi})$$

$$b = - k \Phi \beta$$

The roots of (38) are found via the closed form solution to a cubic. Matsuno discusses several of the lowest modes. Only the $\eta = 0$ mode will be considered in the following evaluation.

An explicit formulation of (35) is

$$\begin{aligned}
 u^{n+1} &= u^{n-1} - U \frac{\Delta t}{\Delta x} \left(u_{j+1}^n - u_{j-1}^n \right) + 2\beta m \Delta y \Delta t v^n \\
 &\quad - \frac{\Delta t}{\Delta x} \left(\phi_{j+1}^n - \phi_{j-1}^n \right) \\
 v^{n+1} &= v^{n-1} - U \frac{\Delta t}{\Delta x} \left(v_{j+1}^n - v_{j-1}^n \right) - 2\beta m \Delta y \Delta t u^n \\
 &\quad - \frac{\Delta t}{\Delta y} \left(\phi_{m+1}^n - \phi_{m-1}^n \right) \\
 \phi^{n+1} &= \phi^{n-1} - U \frac{\Delta t}{\Delta x} \left(\phi_{j+1}^n - \phi_{j-1}^n \right) - \phi \frac{\Delta t}{\Delta x} \left(u_{j+1}^n - u_{j-1}^n \right) \\
 &\quad - \phi \frac{\Delta t}{\Delta y} \left(v_{m+1}^n - v_{m-1}^n \right)
 \end{aligned} \tag{39}$$

The analytic phase frequencies have no y dependence and we anticipate that the frequencies of the numerical scheme do not either. As was pointed out in Section 2, in this problem it is not strictly correct to replace y by $m\Delta y$ in the form of the solution because the functional form of the derivatives will be inconsistent. This may cause the frequency derived for the finite differenced set of equations to depend on y . This difficulty in obtaining a consistent solution form illustrates a limitation of this analysis method. However, we will use the form consistent solution form illustrates a limitation of this analysis method. However, we will use the form

$$\exp \left\{ \frac{-\beta m^2 \Delta y^2}{2\sqrt{\Phi}} + i (kj\Delta x - \omega n \Delta t) \right\} \quad (40)$$

which corresponds to the first, $\eta = 0$, mode of the analytical solution. We will consider this approximation reasonable, if we obtain phase frequencies that vary only by a minute amount with y . This would indicate that (40) is very close to the correct solution. If the y dependence turned out to be strong, then an eigenvector analysis (see Appendix 2) would be required.

After substitution of the form (40), and considerable algebraic manipulation, one obtains the cubic equation

$$D^3 + aD + b = 0$$

where

$$D = \sin \omega \Delta t - U \frac{\Delta t}{\Delta x} \sin k \Delta x$$

$$c = - \frac{\beta \Delta y^2}{2\sqrt{\Phi}}$$

$$a = - \left[\Phi \frac{\Delta t^2}{\Delta x^2} \sin^2 k \Delta x + \beta^2 \Delta t^2 m^2 \Delta y^2 + (1 - e^{4c} \cosh(4cm)) \Phi \frac{\Delta t^2}{2\Delta y^2} \right]$$

$$b = \beta \Delta t \Delta y \Phi \frac{\Delta t}{\Delta x} \sin k \Delta x e^c \cosh(2cm)$$

because β is so small, for a terrestrial problem the dependence of D on y (and therefore of ω_E) is weak. The difference in ω between $m = 0$ and $m = 10$ for $\Delta y = 10^5$ m is in the 4th or larger significant digit, thus our use of (40) is reasonable. The difference in ω between $m = 0$ and $m = 10$ for $\Delta y = 10^5$ m is in the 4th or larger significant digit, thus our use of (40) appears reasonable.

The phase frequencies for the eastward moving gravity wave (E), westward moving gravity wave (W) and Rossby-Haurwitz wave (R) are presented in Figs. 17 and 18. The details of the curves for $0 \leq k\Delta x \leq \pi/20$ are shown in the insert. The rather peculiar behavior of the Rossby-like waves may be due to the use of the approximate solution (40). The analytical roots are complex for values of $\sim 0.01 < k\Delta x < 0.05$ (for $\phi = 10^4 \text{ m}^2 \text{ s}^{-2}$, $\beta = 10^{-11} \text{ m}^{-1} \text{ s}^{-1}$ and $\Delta x = 10^5 \text{ m}$) whereas the numerical frequencies are real; no comparison was made in that range. The Rossby-Haurwitz waves move at about a tenth the speed of the gravity waves, so the linear stability limit, $\Lambda = 1$, is determined by the gravity waves. For small Λ , the explicit and implicit versions are again nearly identical. Therefore, Fig. 17, where $\Lambda \sim 0.5$, is representative of either scheme. The curves have the same basic shape as in previous, simpler, problems. Figure 18 compares the implicit and analytical phase velocities for $\Lambda \sim 5$. The gravity waves are slowed down appreciably, but the much slower Rossby-Haurwitz wave is not appreciably changed by the tenfold increase in Λ .

Since these results are analogous to those from simpler systems it seems reasonable to conclude that they are general properties of the finite difference scheme. That is, one would expect the truncation error of this scheme to have these general properties for similar types. That is, one would expect the truncation error of this scheme to have these general properties for similar types of wave motions.

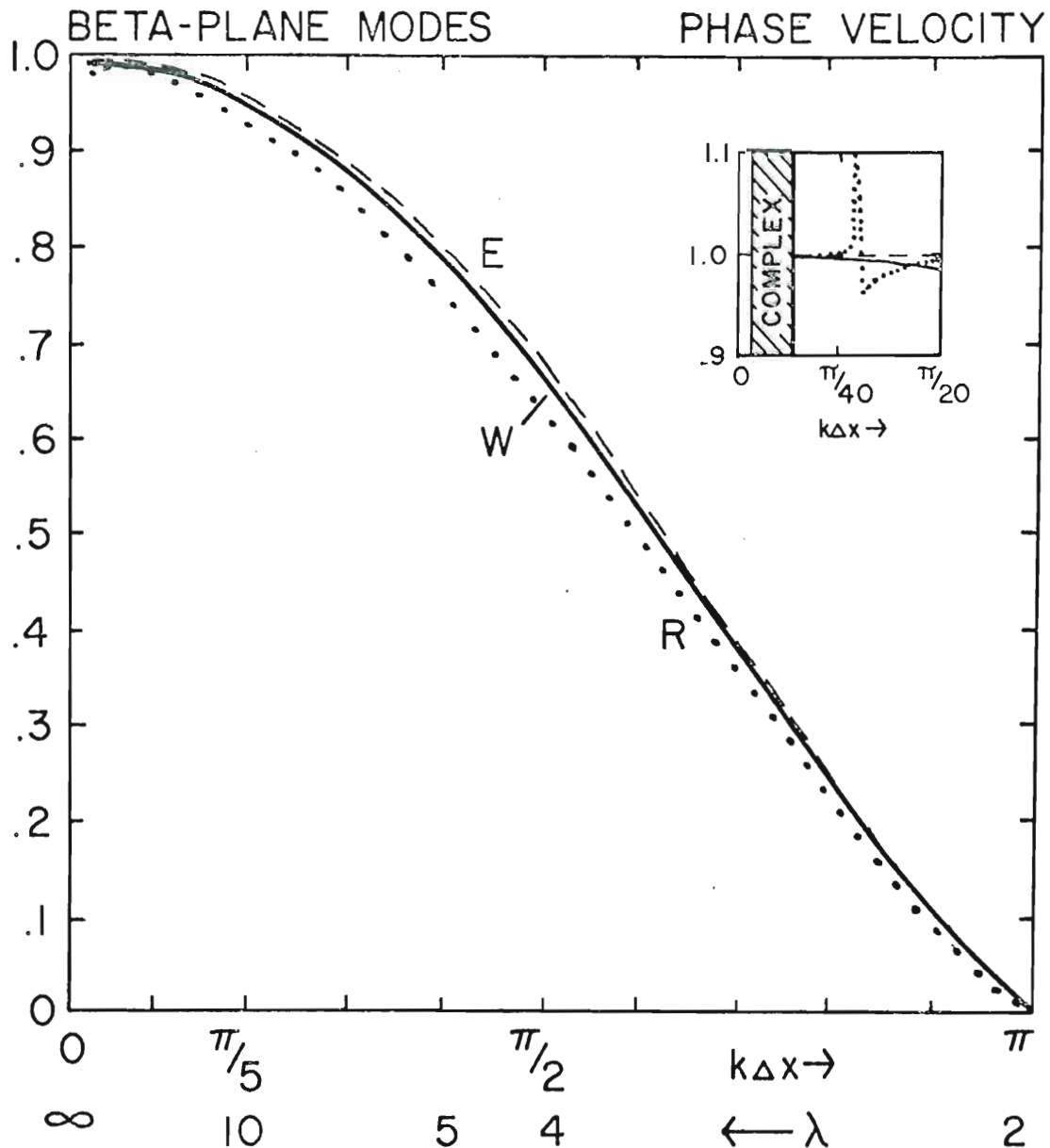


Fig. 17. Phase velocity for the explicit formulation ($\Lambda = 0.5$) of the equatorial β -plane system normalized by the correct speeds. (E) is the eastward propagating gravity wave, (W) the westward propagating gravity wave and (R) the Rossby-Haurwitz wave. The insert shows the details of the error at small values of k . The analytical solution is complex for $\sim 1 \times 10^{-7} < k < 5 \times 10^{-7} \text{ m}^{-1}$ for $\beta = 10^{-11} \text{ m}^{-1} \text{ s}^{-1}$ and $\Phi = 10^4 \text{ m}^2 \text{ s}^{-2}$, here $\Delta x = 10^5 \text{ m}$. The insert shows the details of the error at small values of k . The analytical solution is complex for $\sim 1 \times 10^{-7} < k < 5 \times 10^{-7} \text{ m}^{-1}$ for $\beta = 10^{-11} \text{ m}^{-1} \text{ s}^{-1}$ and $\Phi = 10^4 \text{ m}^2 \text{ s}^{-2}$, here $\Delta x = 10^5 \text{ m}$.

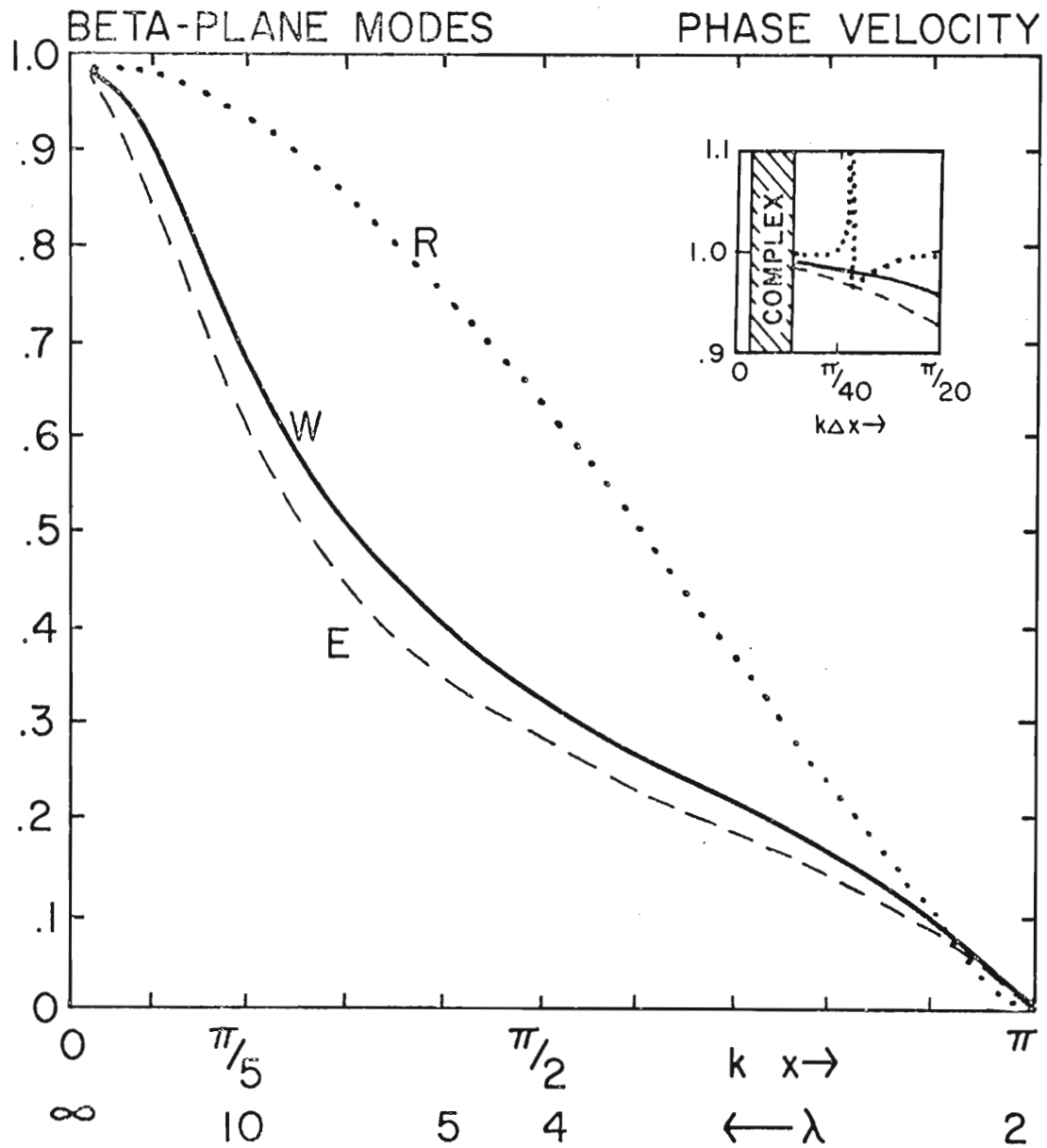


Fig. 18. Same as Fig. 17 but for the implicit scheme at $\Lambda \approx 5$. Note that the tenfold increase in Λ had little effect on the Rossby-Haurwitz waves. These results are consistent with previous results for simpler systems.

Fig. 19. Same as Fig. 17 but for the implicit scheme at $\Lambda \approx 5$. Note that the tenfold increase in Λ had little effect on the Rossby-Haurwitz waves. These results are consistent with previous results for simpler systems.

It would be possible, though tedious, to compute the group velocity for this problem. However, since an approximate solution was used, it may not be appropriate to do so. That is, the misrepresentation caused by using (40) may be magnified by taking the derivative of the numerical frequency solutions.

5. CONCLUSIONS

This study was undertaken to attempt to quantitatively determine the error introduced by finite differencing. Since the field is so broad, testing many schemes, and various boundary and staggered grid formulations was not feasible. Therefore the study was also designed to outline a straightforward method of determining the error which can be applied in practice. The determination is imperative since statements concerning the order of a Taylor series are clearly inadequate to represent the truncation error.

This study confirms several previous results. Namely, that explicit formulations tend to overestimate oscillations whereas implicit formulations underestimate them. Space differencing produces dispersive waves even if the true waves are not dispersive. The phase velocity errors increase as the wavenumber increases, or equivalently, as the number of grid points resolving the wave decreases. Implicit schemes retain stability by slowing down the waves, which is the price extracted for the economy of large time steps. Generally, only the longest waves are handled reasonably well. Several new aspects of the truncation error have been revealed, particularly through comparison of the group velocities. Several new aspects of the truncation error have been revealed, particularly through comparison of the group velocities. The dispersive nature introduced by the finite

differencing causes significant angular, as well as magnitude, errors in the group velocity. Since the group velocity is an indication of the propagation of the energy, this could cause grave dynamical effects in a numerical model, particularly if the short waves carry a significant fraction of the energy. It is also apparent that some of the characteristics of the error evident in simple systems reappear when the same scheme is used in more complex models with similar solutions.

This work examined several linear systems. The intention being, to study the error in the scheme without the additional complications of nonlinear effects. This method could be extended to other types of problems. Further work is currently being considered on formulating boundary and initial conditions based on the interrelationships of variables in the discrete system.

APPENDIX 1

Outline of the method applied to a simple equation

$$\phi_t + U\phi_x + V\phi_y = 0 \quad (\text{A1.1})$$

insert

$$\phi = A e^{i(kx + \ell y - \omega t)}$$

into (A1.1) and

$$-i\omega + ikU + i\ell V = 0$$

$$\omega = Uk + V\ell$$

An explicit formulation of (A1.1) is

$$\phi^{n+1} = \phi^{n-1} - U \frac{\Delta t}{\Delta x} \left[\phi_{j+1}^n - \phi_{j-1}^n \right] - V \frac{\Delta t}{\Delta y} \left[\phi_{m+1}^n - \phi_{m-1}^n \right] \quad (\text{A1.2})$$

use a solution

$$\phi = A e^{i(kj\Delta x + \ell m\Delta y - \omega n\Delta t)} \quad (\text{A1.3})$$

which, when inserted into (A1.2), reduces to

$$e^{-i\omega\Delta t} = e^{i\omega\Delta t} - U \frac{\Delta t}{\Delta x} \left[e^{ik\Delta x} - e^{-ik\Delta x} \right] - V \frac{\Delta t}{\Delta y} \left[e^{i\ell\Delta y} - e^{-i\ell\Delta y} \right]$$

using Euler's relations:

$$\sin \omega\Delta t = U \frac{\Delta t}{\Delta x} \sin k\Delta x + V \frac{\Delta t}{\Delta y} \sin \ell\Delta y$$

thus, for the explicit scheme (A1.2)

thus, for the explicit scheme (A1.2)

$$\omega_E = \frac{1}{\Delta t} \arcsin \left[U \frac{\Delta t}{\Delta x} \sin k\Delta x + V \frac{\Delta t}{\Delta y} \sin \ell\Delta y \right]$$

An implicit scheme for (A1.1) is

$$\begin{aligned} \phi^{n+1} = \phi^n - U \frac{\Delta t}{4\Delta x} & \left(\phi_{j+1}^n + \phi_{j+1}^{n+1} - \phi_{j-1}^n - \phi_{j-1}^{n+1} \right) \\ & - V \frac{\Delta t}{4\Delta y} \left(\phi_{m+1}^n + \phi_{m+1}^{n+1} - \phi_{m-1}^n - \phi_{m-1}^{n+1} \right) \end{aligned}$$

in a similar fashion, substitution of (A1.3) yields

$$\sin \frac{\omega \Delta t}{2} = U \frac{\Delta t}{4\Delta x} \left(2 \cos \frac{\omega \Delta t}{2} \sin k\Delta x \right) + V \frac{\Delta t}{4\Delta y} \left(2 \cos \frac{\omega \Delta t}{2} \sin \ell \Delta y \right)$$

and

$$\omega_I = \frac{2}{\Delta t} \arctan \left[U \frac{\Delta t}{2\Delta x} \sin k\Delta x + V \frac{\Delta t}{2\Delta y} \sin \ell \Delta y \right]$$

APPENDIX 2

Analytic solutions for the beta-plane primitive equations are derived. The more vigorous eigenvector analysis is sketched.

Analytic Beta-Plane Solutions

Given:

$$u_t + Uu_x = fv - \phi_x$$

$$v_t + Uv_x = -fu - \phi_y$$

$$\phi_t + U\phi_x + \Phi(u_x + v_y) = 0$$

substitute solutions for u , v and ϕ of the form

$$F(y) e^{i(kx - \omega t)}$$

where the y variation is left unspecified. Then

$$-iAu = \beta yv - ik\phi \quad (A2.1)$$

$$-iAv = -\beta yu - \frac{\partial \phi}{\partial y} \quad (A2.2)$$

$$-iA\phi + i\Phi ku + \Phi \frac{\partial v}{\partial y} = 0 \quad (A2.3)$$

where

$$A = \omega - Uk$$

Take $\partial/\partial y$ (A2.3), substitute that into (A2.2), and multiply by iA ;

$$iA (-iAv + \beta yu) + ik\Phi \frac{\partial u}{\partial y} + \Phi \frac{\partial^2 v}{\partial y^2} = 0 \quad (A2.4)$$

$$iA (-iAv + \beta yu) + ik\Phi \frac{\partial u}{\partial y} + \Phi \frac{\partial^2 v}{\partial y^2} = 0 \quad (A2.4)$$

Eliminate ϕ between (A2.1) and (A2.3): multiply (A2.1) by A and (A2.3) by k, add;

$$-iA^2u - \beta yAv + i\phi k^2u + \phi k \frac{\partial v}{\partial y} = 0 \quad (\text{A2.5})$$

Eliminate ϕ between (A2.1) and (A2.2) to get;

$$iA \frac{\partial u}{\partial y} + i\beta yku + Akv + \beta y \frac{\partial v}{\partial y} + \beta v = 0 \quad (\text{A2.6})$$

Eliminate $\partial v/\partial y$ term between (A2.5) and (A2.6):

$$-iA^2\beta yu - \beta^2 y^2 Av - ikA\phi \frac{\partial u}{\partial y} - A\phi k^2v - \beta\phi kv = 0 \quad (\text{A2.7})$$

Use (A2.7) as a relation for

$$iA\beta yu - ik\phi \frac{\partial u}{\partial y}$$

Substitute that into (A2.4), and obtain

$$\frac{\partial^2 v}{\partial y^2} + \left(\frac{A^2}{\phi} - k^2 - \frac{\beta k}{A} - \frac{\beta^2 y^2}{\phi} \right) v = 0 \quad (\text{A2.8})$$

let

$$v(y) = G(y) e^{-\frac{1}{2} \frac{\beta}{\sqrt{\phi}} y^2}$$

substitute this into (A2.8):

$$G'' - \frac{2\beta y}{\sqrt{\phi}} G' + \left(\frac{A^2}{\phi} - k^2 - \frac{\beta k}{A} - \frac{\beta^2 y^2}{\phi} \right) G = 0 \quad (\text{A2.9})$$

Assume G is polynomial:

$$G = \sum_{\eta=0}^{\infty} C_{\eta} y^{\eta}$$

Insert this into (A2.9) to obtain the recursion formula:

$$C_{\eta+2} = -C_{\eta} \frac{\left(\frac{A^2}{\phi} - k^2 - \frac{\beta k}{A} - \frac{\beta}{\sqrt{\phi}} - 2 \frac{\beta}{\sqrt{\phi}} \eta \right)}{(n+2)(n+1)} \quad (\text{A2.10})$$

For large η ,

$$\frac{C_{\eta+2}}{C_{\eta}} \sim \frac{2\beta}{\eta\sqrt{\Phi}}$$

thus

$$G \sim \sum_{\eta=0}^{\infty} \frac{2\beta y^{\eta}}{\sqrt{\Phi} \eta!}$$

Thus for finite v at large y , G must be truncated. For each value of η there will be a dispersion relation, obtained from the recursion formula (A2.10):

$$2\eta + 1 = \frac{A^2}{\sqrt{\Phi}\beta} - \frac{k^2\sqrt{\Phi}}{\beta} - \frac{k\sqrt{\Phi}}{A} \quad (\text{A2.11})$$

or

$$A^3 - A(k^2\Phi + (2\eta+1)\beta\sqrt{\Phi}) - k\Phi\beta = 0 \quad (\text{A2.12})$$

Note that if (A2.12) is written

$$A^3 - aA + b = 0$$

then $\frac{a^3}{27} + \frac{b^2}{4} < 0$ and the roots are real, so

$$\omega_i = Uk + A_i$$

(except for a small range of k : $1.3 \times 10^{-7} \text{ m}^{-1} \lesssim k \lesssim 5 \times 10^{-7} \text{ m}^{-1}$ where the roots are complex, for $\Phi = 10^4 \text{ m}^2 \text{ s}^{-2}$ and $\beta = 10^{-11} \text{ m}^{-1} \text{ s}^{-1}$.)

Numerical Beta Plane Solutions

An explicit formulation is

$$u^{n+1} = u^{n-1} - U \frac{\Delta t}{\Delta x} \left(u_{j+1}^n - u_{j-1}^n \right) + 2\beta m \Delta y \Delta t v^n$$

$$u^{n+1} = u^{n-1} - U \frac{\Delta t}{\Delta x} \left(u_{j+1}^n - u_{j-1}^n \right) + 2\beta m \Delta y \Delta t v^n \\ - \frac{\Delta t}{\Delta x} \left(\phi_{j+1}^n - \phi_{j-1}^n \right)$$

$$\begin{aligned}
v^{n+1} &= v^{n-1} - U \frac{\Delta t}{\Delta x} \left(v_{n+1}^n - v_{n-1}^n \right) - 2\beta m \Delta y \Delta t u^n \\
&\quad - \frac{\Delta t}{\Delta y} \left(\phi_{m+1}^n - \phi_{m-1}^n \right) \\
\phi^{n+1} &= \phi^{n-1} - U \frac{\Delta t}{\Delta x} \left(\phi_{j+1}^n - \phi_{j-1}^n \right) - \phi \frac{\Delta t}{\Delta x} \left(u_{j+1}^n - u_{j-1}^n \right) \\
&\quad - \phi \frac{\Delta t}{\Delta y} \left(v_{m+1}^n - v_{m-1}^n \right)
\end{aligned}$$

where $y = m\Delta y$.

Though the y varying part of the solution is not strictly correct, we will use a solution of the form

$$v = \exp \left\{ \frac{-\beta (m\Delta y)^2}{2\sqrt{\Phi}} + i (kj\Delta x - \omega n\Delta t) \right\}$$

$$u = Av \quad \text{and} \quad \phi = Bv$$

where the arbitrary coefficients, A and B will be eliminated. The correct solution form can be numerically found through an eigenvector analysis, this will be sketched later. Insert the solution forms into the explicit formulation to obtain:

$$\begin{aligned}
-2iA \sin \omega \Delta t &= -2iA U \frac{\Delta t}{\Delta x} \sin k\Delta x + 2\beta m \Delta y \Delta t \\
&\quad - \frac{\Delta t}{\Delta x} 2i B \sin k\Delta x \quad (A2.13)
\end{aligned}$$

$$\begin{aligned}
-2i \sin \omega \Delta t &= -2i U \frac{\Delta t}{\Delta x} \sin k\Delta x - 2\beta m \Delta y \Delta t A \\
&\quad - \frac{\Delta t}{\Delta y} \left\{ B_{m+1} \exp (C(m+1)^2) \right\} \\
&\quad - \frac{\Delta t}{\Delta y} \left\{ B_{m+1} \exp (C(m+1)^2) \right\} \\
&\quad - B_{m-1} \exp [C(m-1)^2] \Big] e^{-Cm^2} \quad (A2.14)
\end{aligned}$$

$$\begin{aligned}
 - 2i B \sin \omega \Delta t &= - 2i U \frac{\Delta t}{\Delta x} B \sin k \Delta x - 2i \phi \frac{\Delta t}{\Delta x} A \sin k \Delta x \\
 &- \phi \frac{\Delta t}{\Delta y} \left[\exp \{C(m+1)^2\} - \exp \{C(m-1)^2\} \right] e^{-Cm^2}
 \end{aligned}
 \tag{A2.15}$$

where

$$C \equiv \frac{\beta \Delta y^2}{2 \sqrt{\phi}}$$

If we define:

$$E \equiv \frac{\Delta t}{\Delta x} \sin k \Delta x$$

$$D \equiv \sin \omega \Delta t - UE$$

$$F' \equiv \beta \Delta y \Delta t, \quad F = F'm$$

$$G \equiv 2e^C \sinh (2 cm)$$

then (A2.13) and (A2.15) can be written

$$- 2i AD = 2F - 2iBE$$

$$- 2i BD = - 2i \phi EA - \phi \frac{\Delta t}{\Delta y} G$$

Solving for A and B, one obtains

$$A = \frac{i \left[FD - E \phi \frac{\Delta t}{2 \Delta y} G \right]}{D^2 - \phi E^2}$$

$$B = \frac{i \left[\phi EF - \phi D \frac{\Delta t}{2 \Delta y} G \right]}{D^2 - \phi E^2}$$

Insert these relations into (A2.14), and after some manipulation derive the cubic equation in D:

Derivation of the cubic equation in D:

$$\begin{aligned}
 D^3 + \left[-\phi E^2 - F^2 - (1 - e^{4C} \cosh (4 cm)) \phi \frac{\Delta t^2}{2 \Delta y^2} \right] D \\
 - F' \phi E \frac{\Delta t}{\Delta y} e^C \cosh (2 cm) = 0
 \end{aligned}
 \tag{A2.16}$$

which is of the form

$$D^3 + aD + b = 0$$

If the quantity

$$\frac{a^3}{27} + \frac{b^2}{4} < 0$$

then the roots are given by

$$\begin{aligned} r_1 &= 2 (-a/3)^{1/2} \cos (\phi/3) \\ r_2 &= 2 (-a/3)^{1/2} \cos (\phi/3 + 2\pi/3) \\ r_3 &= 2 (-a/3)^{1/2} \cos (\phi/3 + 4\pi/3) \end{aligned} \quad (\text{A2.17})$$

where

$$\phi \equiv \arccos \left(-b / \left(2(-a^3/27)^{1/2} \right) \right)$$

The relations (A2.17) are used to determine the phase frequencies, through the relation

$$\omega_i = \frac{1}{\Delta t} \arcsin \left\{ UE + r_i \right\} \quad (\text{A2.18})$$

Matrix Formulation

As an alternative, and more rigorous, method, the frequencies can be found from the eigenvector. One proceeds in an analogous fashion as for the continuous system of equations by first keeping the y variation arbitrary. Thus the explicit formulation is written:

$$\begin{aligned} -2i Du_m &= 2FV_m - 2iE\phi_m \\ -2i Du_m &= 2FV_m - 2iE\phi_m \\ -2i D\phi_m &= -2i \phi E u_m - \phi \frac{\Delta t}{\Delta y} (v_{m+1} - v_{m-1}) \end{aligned}$$

for the x momentum and continuity equations.

Eliminate for u_m and ϕ_m :

$$\phi_m = \frac{2F\phi E v_m - D\phi \frac{\Delta t}{\Delta y} (v_{m+1} - v_{m-1})}{2i (D^2 - \phi E^2)}$$

$$u_m = \frac{2FDv_m - \phi E \frac{\Delta t}{\Delta y} (v_{m+1} - v_{m-1})}{2i (D^2 - \phi E^2)}$$

Insert these into the y momentum equation

$$2i Dv_m = 2Fu_m + \frac{\Delta t}{\Delta y} (\phi_{m+1} - \phi_{m-1})$$

to obtain:

$$\begin{aligned} -4v_m D (D^2 - \phi E^2) &= 2F \left[2FDv_m - \phi E \frac{\Delta t}{\Delta y} (v_{m+1} - v_{m-1}) \right] \\ &+ \frac{\Delta t}{\Delta y} \left[2F\phi E (v_{m+1} - v_{m-1}) - \phi D \frac{\Delta t}{\Delta y} (v_{m+2} + v_{m-2} - 2v_m) \right] \end{aligned}$$

which is a pentdiagonal system of the form:

$$Av_{m+2} + Bv_m + Av_{m-2} = 0$$

where

$$A = \phi D \frac{\Delta t^2}{\Delta y^2}$$

$$B = -4D (D^2 - \phi E^2 - F^2) + 2\phi D \frac{\Delta t^2}{\Delta y^2}$$

away from the boundaries in y.

From this matrix the eigenvalues are determined and the frequencies derived.

To clarify one might define a matrix N which contains the frequencies derived.

To clarify, one might define a matrix, N, which contains no D's as

$$M + P(D) = N$$

where P is a function of D , for example a cubic. N will contain known quantities (ω , contained only in D , is the sole unknown). Then $P(D) =$ eigenvalues of N , and the frequencies can be found. Note that if the eigenvalues must be found numerically, it is not necessarily clear which frequency of the numerical system corresponds to a frequency of the continuous system.

REFERENCES

- Baer, F., and T. J. Simmons, 1970: Computational stability and time truncation of coupled nonlinear equations with exact solutions. Mon. Wea. Rev., 98, 665-679.
- Blumen, W., 1972: Geostrophic adjustment. Rev. Geophys., 10, 485-528.
- Charney, J. G., R. Fjörtoft, and J. von Neumann, 1950: Numerical integration of the barotropic vorticity equation. Tellus, 2, 237-254.
- Courant, R., K. O. Friedrichs, and H. Lewy, 1928: Über die Partiiellen Differenzen gleichungen der Mathematischen Physik. Math. Annal., 100, 32-74. Translated, 1967, IBM Jour., 215-234.
- Elvius, T., and A. Sundström, 1973: Computationally efficient schemes and boundary conditions for a fine-mesh barotropic model based on the shallow-water equations. Tellus, 25, 132-156.
- Gates, W. L., 1959: On the truncation error, stability, and convergence of difference solutions of the barotropic vorticity equation. J. Meteor., 16, 556-568.
- _____, and C. A. Riegel, 1962: A study of numerical errors in the integration of barotropic flow on a spherical grid. J. Geophys. Res., 67, 773-784.
- Grammelvedt, A., 1969: A survey of finite difference schemes for the primitive equations for a barotropic fluid. Mon. Wea. Rev., 97, 384-404.
- Kurihara, Y., 1965: On the use of implicit and iterative methods for the time integration of the wave equation. Mon. Wea. Rev., 93, 33-46.
- Kwizak, M., 1970: Semi-implicit integration of a grid point model of the primitive equations. Pub. in Meteorology No. 98, Arctic Met. Res. Group, McGill Univ.
- _____, 1970: A semi-implicit integration of a grid point model of the primitive equations. Pub. in Meteorology No. 98, Arctic Met. Res. Group, McGill Univ.

- Kreiss, H., and J. Olinger, 1972: Comparison of accurate methods for the integration of hyperbolic equations. Tellus, 24, 199-215.
- Lindzen, R. D., 1967: Planetary waves on beta-planes. Mon. Wea. Rev., 95, 441-451.
- Matsuno, T., 1966: Quasi-geostrophic motions in the equatorial area. J. Meteor. Soc. Japan, 44, 25-43.
- Miles, J. W., 1974: On Laplace's tidal equations. J. Fluid Mech., 66, 241-260.
- Orzag, S. A., 1971: Numerical simulation of incompressible flows within simple boundaries: Accuracy. J. Fluid Mech., 49, 75-112.
- Whitham, G. B., 1974: Linear and nonlinear waves. John Wiley and Sons, 636 pp.
- Young, J. A., 1968: Comparative properties of some time differencing schemes for linear and nonlinear oscillations. Mon. Wea. Rev., 96, 357-364.

VITA

Richard Grotjahn was born September 1, 1951 in Seattle, Washington. In June 1973 he graduated from the University of Washington with a B.S. degree in Atmospheric Sciences. He began his graduate study in the Department of Meteorology at the Florida State University in September 1973. He was a participant in the 1974 Summer Fellowship Program in Scientific Computing at the National Center for Atmospheric Research.